




Chronology of subduction and collision along the İzmir-Ankara suture in Western Anatolia: records from the Central Sakarya Basin

Faruk Ocakođlu, Aynur Hakyemez, Sanem Aıkalin, Sevin Özkan Altiner, Yeřim Büyükmeri, Alexis Licht, Huriye Demircan, Ümit řafak, Ayřegöl Yıldız, İsmail Ömer Yılmaz, Michael Wagreich & Clay Campbell


To cite this article: Faruk Ocakođlu, Aynur Hakyemez, Sanem Aıkalin, Sevin Özkan Altiner, Yeřim Büyükmeri, Alexis Licht, Huriye Demircan, Ümit řafak, Ayřegöl Yıldız, İsmail Ömer Yılmaz, Michael Wagreich & Clay Campbell (2018): Chronology of subduction and collision along the İzmir-Ankara suture in Western Anatolia: records from the Central Sakarya Basin, International Geology Review, DOI: [10.1080/00206814.2018.1507009](https://doi.org/10.1080/00206814.2018.1507009)

To link to this article: <https://doi.org/10.1080/00206814.2018.1507009>

 View supplementary material 

 Published online: 22 Aug 2018.

 Submit your article to this journal 

 Article views: 58

 View Crossmark data 

Chronology of subduction and collision along the İzmir-Ankara suture in Western Anatolia: records from the Central Sakarya Basin

Faruk Ocakoğlu^a, Aynur Hakyemez^b, Sanem Açıkalin^c, Sevinç Özkan Altiner^d, Yeşim Büyükmeriç^e, Alexis Licht^f, Huriye Demircan^b, Ümit Şafak^g, Ayşegül Yıldız^h, İsmail Ömer Yılmaz^d, Michael Wagreichⁱ and Clay Campbell^j

^aDepartment of Geological Engineering, Eskişehir Osmangazi University, Eskişehir, Turkey; ^bDepartment of Geological Research, General Directorate of Mineral Research and Exploration (MTA), Ankara, Turkey; ^cDepartment of Civil Engineering and Geosciences, Newcastle University, Newcastle, UK; ^dDepartment of Geological Engineering, Middle East Technical University, Ankara, Turkey; ^eDepartment of Geological Engineering, Bülent Ecevit University, Zonguldak, Turkey; ^fDepartment of Earth and Space Sciences, University of Washington, Seattle, WA, USA; ^gDepartment of Geological Engineering, Çukurova University, Adana, Turkey; ^hDepartment of Geological Engineering, Aksaray University, Aksaray, Turkey; ⁱDepartment for Geodynamics and Sedimentology, University of Vienna, Vienna, Austria; ^jDepartment of Geology, University of Kansas, Lawrence, KS, USA

ABSTRACT

Western Anatolia is a complex assemblage of terranes, including the Sakarya Terrane and the Tauride-Anatolide Platform that collided during the late Cretaceous and Palaeogene (80–25 Ma) after the closure of the İzmir-Ankara Ocean. Determining the precise timing at which this ocean closed is particularly important to test kinematic reconstructions and geodynamic models of the Mediterranean region, and the chronology of suturing and its mechanisms remain controversial. Here, we document the Cretaceous-Eocene sedimentary history of the Central Sakarya Basin, along the northern margin of the Neotethys Ocean, via various approaches including biostratigraphy, geochronology, and sedimentology. Two high-resolution sections from the Central Sakarya Basin show that pelagic carbonate sedimentation shifted to rapid siliciclastic deposition in the early Campanian (~ 79.6 Ma), interpreted to be a result of the build-up of the accretionary prism at the southern margin of the Sakarya Terrane. Rapid onset of deltaic progradation and an increase in accumulation rates in the late Danian (~ 61 Ma), as well as a local angular unconformity are attributed to the onset of collision between the Sakarya Terrane and the Tauride-Anatolide Platform. Thus, our results indicate that though deformation of the subduction margin in Western Anatolia started as early as the Campanian, the closure of the İzmir-Ankara Ocean was only achieved by the early Palaeocene.

ARTICLE HISTORY

Received 30 April 2018
Accepted 29 July 2018

KEYWORDS

Basin subsidence; biostratigraphy; collision; İzmir-Ankara Suture; sediment flux; tectonics and sedimentation

1. Introduction

Early regional geological syntheses of Turkey (e.g., Saner 1980; Şengör and Yılmaz 1981) have shown that Central Anatolia is a complex assemblage of terranes, including the Pontides to the north, and the Tauride-Anatolide Platform to the south, separated by the ca. 2000 km long İzmir-Ankara-Erzincan Suture Zone (Okay and Tüysüz 1999). Three decades of geological studies including stratigraphic, sedimentological, and tectonic approaches, as well as the application of more up-to-date studies of magmatic geochemistry, geochronology, metamorphism, palaeomagnetism, and geophysics have enabled a robust and increasingly refined evolutionary picture of the Anatolian Orogeny and of its different terranes (e.g., Altiner *et al.* 1991; Tüysüz 1999; Göncüoğlu *et al.* 2000; Okay *et al.* 2001; Robertson and

Ustaömer 2004; Okay 2008; Genç and Tüysüz 2010; Göncüoğlu *et al.* 2010; Altunkaynak and Dilek 2013).

The outline of the gross geological picture can be summarized as follows:

- (1) The Sakarya Zone occupied the southernmost part of the Scythian Platform in the late Jurassic-earliest Cretaceous, which is the southern prolongation of the East European Craton (Okay *et al.* 2013)
- (2) Rifting of the Pontides from the Laurasian margin during the opening of the proto-Black Sea, and further division of the Pontides into two microcontinents, the Sakarya and the İstanbul terranes, which were separated by the Intra-Pontide Ocean, where the timing of opening and suturing remain debated (Şengör and Yılmaz 1981;

- Altiner *et al.* 1991; Göncüoğlu *et al.* 2000; Göncüoğlu *et al.* 2014)
- (3) Onset of the closure of the northern branch of the Neotethys by means of two north-vergent subduction zones, one intra-oceanic, the other beneath the southern Pontides margin (Göncüoğlu *et al.* 2010), and development of a magmatic arc on the Pontides (Okay *et al.* 2001)
 - (4) Development of the HP-LT Tavşanlı Zone in the frontal part of the Anatolide-Tauride Platform in the Cenonian-early Campanian as a result of continental subduction created by the closure of the intra-oceanic subduction zone (Okay 1984; Okay *et al.* 1998; Sherlock *et al.* 1999)
 - (5) Collision of the Anatolide-Tauride Platform with the Pontides during the late Cretaceous-early Eocene and closure of the northern branch of the Neotethys along the İzmir-Ankara-Suture Zone (Okay and Tüysüz 1999)
 - (6) Development of early-middle Eocene magmatism related to slab-break-off beneath the Sakarya Terrane (Altunkaynak and Dilek 2013; Kasapoğlu *et al.* 2016).

Timing of suturing and collision along the İzmir-Ankara Suture has been hotly debated in the literature and remains a controversial issue, with closure estimates varying from the late Cretaceous to the early Eocene (Göncüoğlu *et al.* 1996; Okay *et al.* 2001; Okay and Satır 2006; Leren *et al.* 2007; Okay 2008; Meijers *et al.* 2010). In Central Anatolia, palaeomagnetic data demonstrate that collision along the southern margin of the Central Pontides started in the latest Cretaceous to early Palaeocene causing oroclinal bending (Channell *et al.* 1996; Meijers *et al.* 2010). The convergence ensued throughout the Eocene and Oligocene resulting in further deformation and rotation throughout the suture zone, marked by the shift to foreland basin deposition in the Palaeocene (Oçakoğlu 1995; Nairn *et al.* 2013; Licht *et al.* 2017). Deformation reached the northern Central Pontide basins in the early Eocene (Leren *et al.* 2007; Hippolyte *et al.* 2010, 2015; Çinku *et al.* 2011). There is further stratigraphic and structural evidence from the Central Pontides indicating that the collision started in the late Palaeocene-early Eocene under the control of strike slip deformation, however this convergence has alternately been interpreted to be related to closure of the Intra-Pontide Suture (Catanzariti *et al.* 2013; Ottria *et al.* 2017). As for West Anatolia, onset of the collision has been suggested as either the early Palaeocene (Okay *et al.* 2001; Okay and Satır 2006) or the late Palaeocene-

early Eocene (Okay 2008). Therefore, understanding the chronology of the collision is particularly important in order to test kinematic reconstructions, geodynamic models and palaeo-biogeographic scenarios of the Mediterranean region.

In the western Sakarya Terrane there is a narrow (~ 100 km from north to south) and elongated basin (~ 300 km from Bilecik in the west to the Miocene Galatian Massif in the east) parallel to Turkey's principal suture zone (Figure 1; Okay *et al.* 2001). This basin has various names (Mudurnu-Göynük Basin, Central Sakarya Basin) in the literature and here we prefer the Central Sakarya Basin (CSB) proposed by Altınlı (1976) for its geographical and geological connotations. The thick (~ 5 km) Mesozoic-Lower Cenozoic sedimentary sequence of this basin has been the subject of many individual, however spatially limited stratigraphical and sedimentological studies (see the references in Oçakoğlu *et al.* 2007; Oçakoğlu and Açıkalın 2009). Basin-wide studies are scarce and lack precise geochronological and biostratigraphic constraints (Saner 1980; Şeker and Kesgin 1991; Göncüoğlu *et al.* 1996; Oçakoğlu *et al.* 2007). Geochemical, isotopic and clay mineralogic investigation of the basin-fill have been sparse and focused on the central part of the basin (Oçakoğlu and Açıkalın 2009; Açıkalın *et al.* 2016). These studies have shown that the basin displays frequent lateral and vertical facies changes probably controlled by its tectonic evolution.

The present study proposes a complete reassessment of the stratigraphy and sedimentology of the Upper Cretaceous-Lower Cenozoic sequence of the CSB, based on detailed sedimentary logs spread across the basin and dated with new biostratigraphic (primarily planktonic foraminifera, supplemented by nannofossil, radiolaria, mollusca, and ostracoda biostratigraphy) and geochronological constraints. The reconstructed basin-fill architecture for the CSB provides new insights that allow us to check the validity and timing of convergence events that have been previously hypothesized in the north and south Sakarya Terrane.

2. Geological setting and stratigraphy of the CSB throughout the Upper Jurassic – Palaeogene

The CSB opened in the early to middle Jurassic; however, most of its Jurassic and Cretaceous history is dominated by continental margin pelagic and clastic carbonate sedimentation (Altiner *et al.* 1991; Göncüoğlu *et al.* 2000; Okay *et al.* 2001; Yılmaz *et al.* 2016). During the Cenonian, the Intra-Pontide Ocean, located north of the Sakarya Terrane began to close as northward subduction initiated. Closure of the Intra-

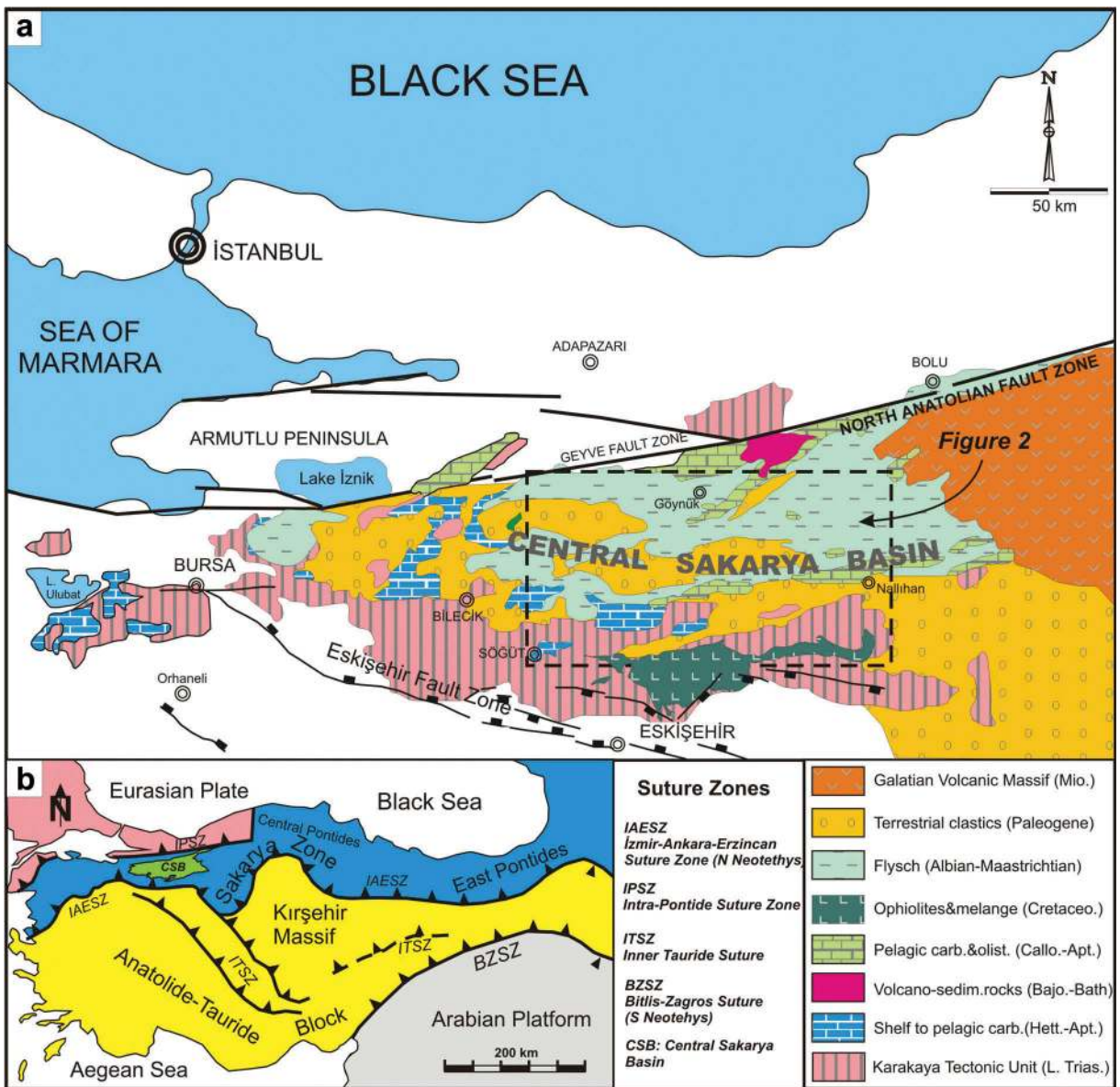


Figure 1. Simplified geological map of the NW Anatolia (A) (revised after Altınır *et al.* 1991; Turhan 2002). Position of the Central Sakarya Basin (CSB) with respect to the main tectonic units of Anatolia (B) (redrawn from Okay and Tüysüz 1999).

Pontide Ocean was complete by the Cenomanian (Tüysüz 1999; Robertson and Ustaömer 2004), as evidenced by associated accretionary complex development and Albian metamorphism (Okay *et al.* 2013) – however, the timing of this closure has been recently challenged (Akbayram *et al.* 2016). Meanwhile, the Neotethys Ocean started subducting northwards below the southern margin of the Sakarya Terrane in the Turonian (Okay *et al.* 2001), and a magmatic arc was active until Campanian times throughout the Pontides (Tüysüz 1999; Okay *et al.* 2001; Karacık and Tüysüz 2010; Özcan *et al.* 2012).

A Geological map (Figure 2) as well as four synthetic stratigraphic columns are used to describe Upper

Jurassic to Eocene sedimentation (Figure 3), compiled from various local studies across the CSB. The first three columns in Figure 3 represent the western, central and eastern parts of the basin while the fourth column belongs to a subbasin that developed during the collisional stage, just in the south of the CSB.

The early to middle Jurassic history of the CSB comprises a terrestrial to shallow marine rift sequence with lesser amounts of volcanic intercalations deposited unconformably above the Variscan basement (Altınır *et al.* 1991; Göncüoğlu *et al.* 2000; Genç and Tüysüz 2010). The Upper Jurassic-Lower Cretaceous succession is dominantly composed of carbonates, and is regarded as the late stage syn-rift basin infill (Altınır *et al.* 1991;

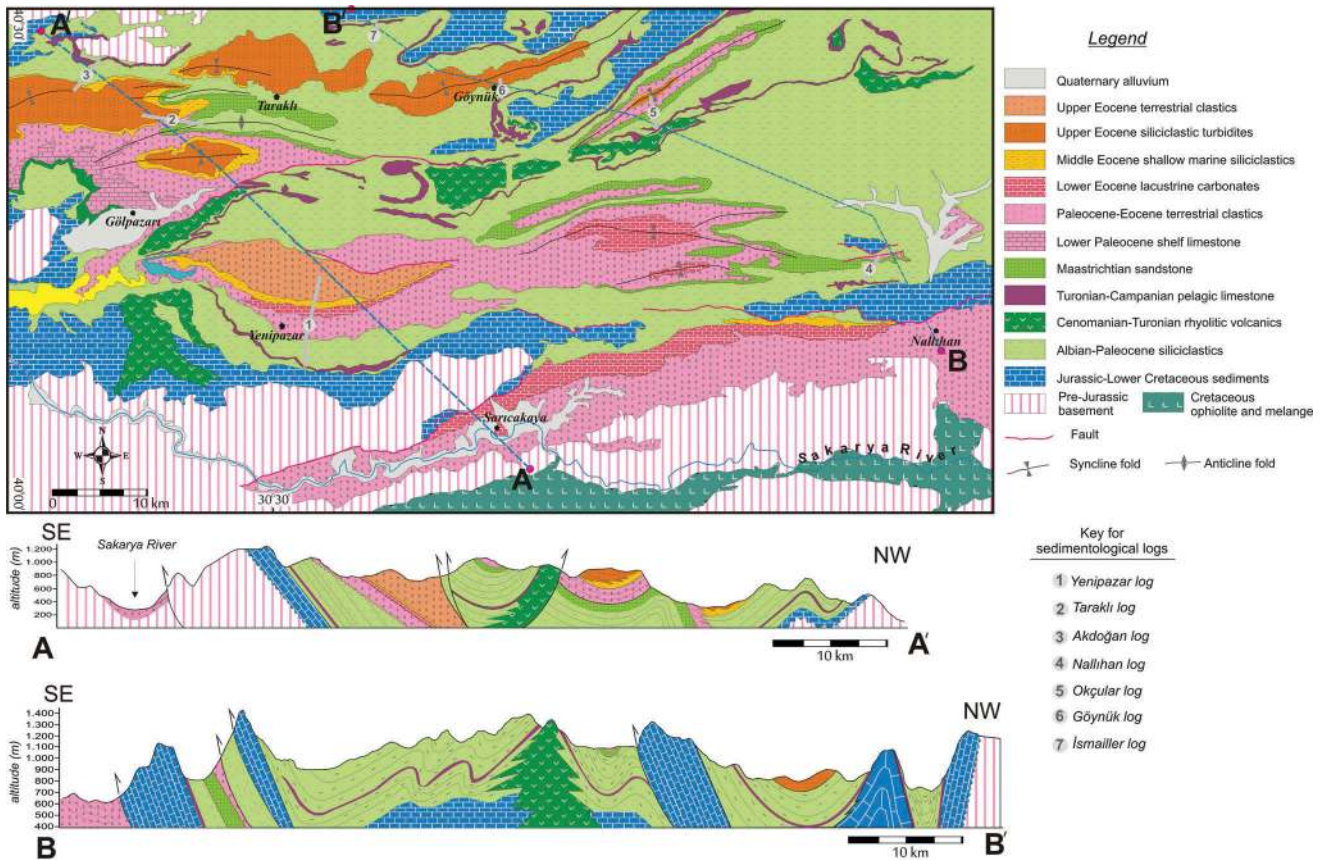


Figure 2. Geological map (simplified after Duru *et al.* (2002), Gedik and Aksay (2002) and Timur and Aksay (2002)), and cross sections of the Central Sakarya Basin.

Koçyiğit *et al.* 1991). In the western portion of the CSB, around the town of Gölpaazarı, shallow marine reefal carbonates (Bilecik fm.) interfinger with the deeper pelagic carbonates (Soğukçam fm.) (Duru *et al.* 2002). Shallow marine carbonates are typically beige to pink coloured, medium to thick bedded and massive, and include varying amounts of corallgal reefal limestone (Granit and Tintant, 1960; Saner 1977, 1980; Duru *et al.* 2002; the references therein). In the central and eastern part of the basin, ammonite-bearing pelagic limestones were deposited in the late Jurassic-early Cretaceous. In the Nallıhan area, based on distinct differences in the limestones' lithofacies and biofacies, the Yosunlukbayırı fm. was divided in to two stratigraphic units (Altıner *et al.* 1991). The lower assemblage of the Yosunlukbayırı fm. spans a time period of Tithonian to Barremian, and is composed of radiolarian-, belemnite- and ammonite-bearing yellowish green clayey limestone, detrital limestone and shale at the base, followed by the upper assemblage, which consists of monotonous detrital limestone at the top (Altıner *et al.* 1991). Further up-section, limestone facies of mudstone and wackstone are observed with abundant slumps, and contain lesser amounts of chert nodules and

calciturbidites, which collectively belong to the Soğukçam fm. Infrequent limestone olistoliths as well as abundant slumps in various levels of the Upper Jurassic-Lower Cretaceous sequence confirm the on-going influence of extensional tectonics during deposition.

Throughout the CSB, the Albian-Campanian time interval is represented by a series of lithological associations with complex architecture whose chronology and source area characterization have been poorly defined until now: Siliciclastic turbidites and pelagic mudstones (Yenipazar and Seben formations), volcanics and exceptionally preserved lava (Üzümlü member), pelagic carbonates (Değirmenözü member) and submarine canyon-fill deposits (Eymür member). The background siliciclastic deposition occurred in a distal to middle lobe setting in the western sector where Jurassic limestone olistoliths locally accompanied deposition (Saner 1977). Alternation of rhyolitic lava, tuff, agglomerate, and intervening siliciclastics of the Üzümlü member record long-lived submarine explosive volcanism (Demirkol 1977; Saner 1977; Göncüoğlu *et al.* 1996) during the Cenomanian across the basin. Up-section, thin-bedded, pink to beige

fossiliferous (radiolarian and planktonic foraminifera) pelagic limestones with tuff intervals deposited in the Santonian-early Campanian (Değirmenözü member) blanket the central and eastern parts of the basin (Saner 1980; Gedik and Aksay 2002; Ocakoğlu *et al.* 2007). Stratigraphically upward, a Campanian terrestrial to shallow marine conglomeratic wedge (Eymür member) is well-developed near Nallıhan and Seben (Kazancı 1979; Önal *et al.* 1988; Şeker and Kesgin 1991), which is linked to an important relative sea-level drop during the mid-Campanian (Ocakoğlu *et al.* 2009, 2013).

In the CSB, facies changes in the N-S direction and the prevalence of a southern sediment source became prominent from the Maastrichtian onwards (Saner 1980; Besbelli 1991). Abundant macro-fossiliferous, medium to thick bedded deltaic sandstones (Taraklı member) and intertongued pelagic limestone intervals with abundant echinoid and planktonic forams (esp. in the Göynük

area) confirm the shoaling of a marine depositional environment (Saner 1977). In the Nallıhan area, Tansel (1980) observed sandstone-conglomerate alternations in this unit and described a late Maastrichtian benthonic foraminifera biozone. The temporal framework of these deltaic sandstones and overlying terrestrial red clastics have been designated quite differently in different parts of the basin (Figure 3), likely due to the lack of geochronological characterization and correlation across the basin as well as E-W lateral facies changes.

Deltaic sandstones are gradually overlain in the E-W direction by terrestrial red clastics (Kızılcay fm.), which interfinger with reefal carbonates (Selvınar fm.) (Altınlı 1976; Saner 1977). The red clastics of the Kızılcay fm., which are dominated by conglomerates and mudstones comprise a separate member consisting of carbonate – shale alternations, known as the Kabalar member. This unit is interpreted to be deposited in a lagoonal setting, based on the brachic to epineritic ostracoda content

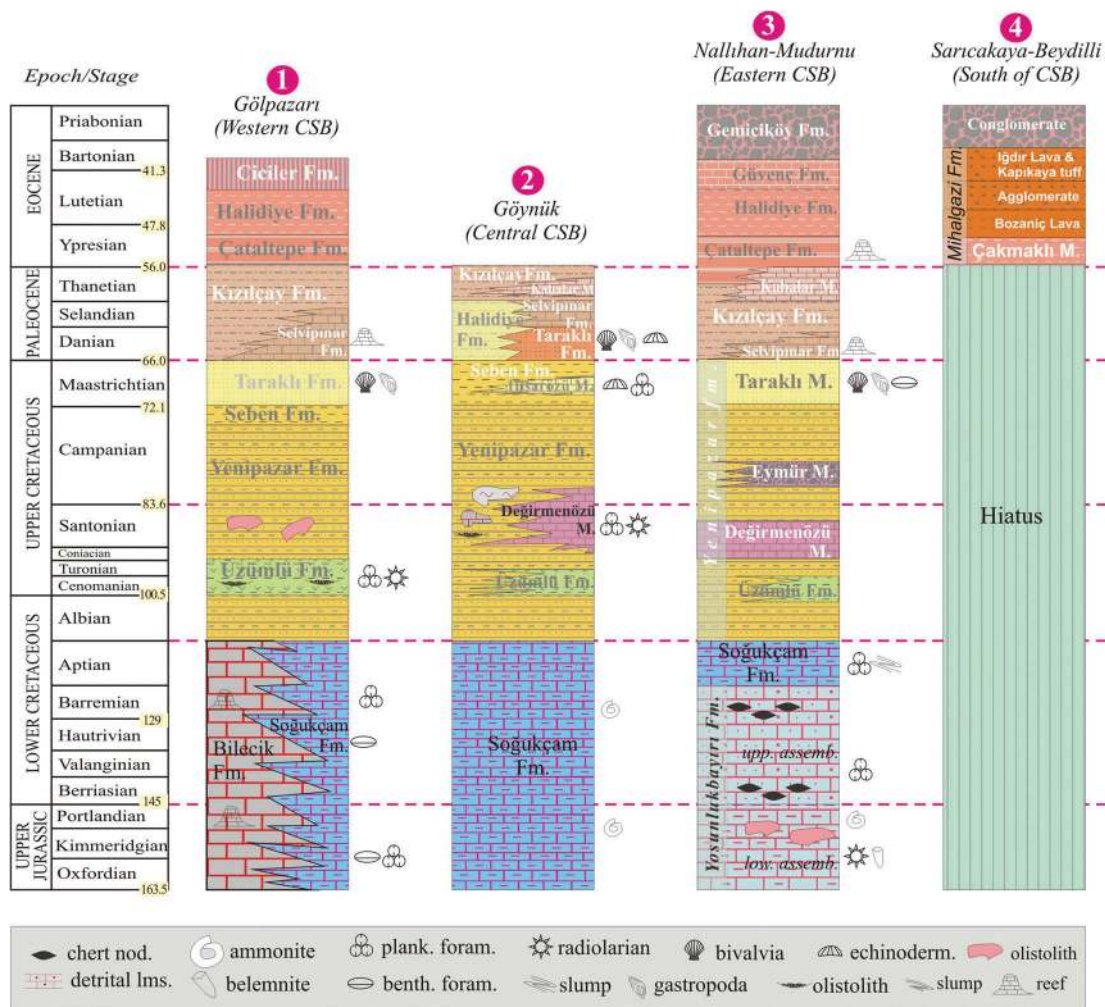


Figure 3. Generalized stratigraphic columns spanning late Jurassic to Eocene from different parts of the Central Sakarya Basin. (1) Saner (1977) and Duru *et al.* (2002), (2) Besbelli (1991) and Gedik and Aksay (2002), (3) Timur and Aksay (2002), Tansel (1980) and Altın *et al.* (1991), and (4) Yıldız *et al.* (2015) and Kasapoğlu *et al.* (2016).

south of the line between Gölpazarı and S. Göynük, which exhibits orbitally driven lithofacies cycles of different temporal hierarchies (Ocakoğlu *et al.* 2012). A marine influence is also suggested based on the geochemical data from oil shale in this unit (Sarı and Aliyev 2005).

In the Eocene, a basin-wide transgression gave rise to the deposition of a shallow marine coarse clastics with abundant molluscs and corals (Çataltepe fm.). The on-going deepening resulted in vertical and lateral facies changes to a sedimentary package composed of alternating thin to medium turbidite beds and hemipelagic muds (Halidiye fm) in an overall shallow marine setting (Saner 1977; Besbelli 1991; Ocakoğlu *et al.* 2007). The youngest marine sediments of the CSB are lithologically highly varied, and predominantly composed of late Lutetian-aged mudstone-fossiliferous limestone alternations (Gedik and Aksay 2002). The youngest conformable unit of the CSB is the Gemiciköy Formation whose outcrops are only preserved north of Yenipazar (Figure 2). This unit gradually overlies Eocene marine clastics (Güvenç fm.), and formed from coarse-grained fluvial deposits. Up-section, the unit increases in the amount and size of reworked blocks from the Cretaceous-Palaeocene basin-fill and the basaltic lava blocks are remarkable (Eroskay 1965; Ocakoğlu *et al.* 2007).

The Sarıcakaya-Beydilli section in Figure 3 represents the terrain north of the south-vergent thrust zone that extends from Sarıcakaya east to Nallıhan (Figure 2). This section is composed of Lower-Middle Eocene terrestrial siliciclastics (Çakmaklı member) and an interfingered volcanic complex, deposited on the Variscan basement (Yıldız *et al.* 2015). The latter is composed of basaltic-andesitic lava flows, andesitic-rhyolitic domes and locally agglomerates and tuffs. Detrital zircon U-Pb ages from this volcanic complex yielded ages between 51 and 47 Ma (Kasapoğlu *et al.* 2016).

3. Methods

We measured 12 sedimentological logs between the Gölpazarı and Nallıhan towns in a 120 km wide area, mostly starting from the Değirmenözü Member (Turonian-Campanian) and extending as far up as possible in to the basin-fill. Thickness of the logs vary from 862 to 2370 m. Each section is of cm-to-dm resolution and encompasses various information such as lithology, sedimentary structure, macro-fossil content, palaeocurrent direction, and samples collected for biostratigraphic and geochronological dating. Here we present seven sedimentological logs, measured along two NW

bearing geotraverses (Figure 2). Although simplified, lithofacies, biostratigraphy and palaeocurrent data are still visible in these sedimentological logs (Figures 4 & 7).

Two volcanoclastic sandstone samples were selected for U-Pb dating of zircons on the Göynük Section. Zircon crystals were extracted by traditional methods of heavy mineral separation at the Department of Geology, University of Kansas. U-Pb ages were generated using laser-ablation inductively coupled plasma mass-spectrometry (LA-ICP-MS) with a laser spot diameter of 20 µm. Detailed methods for extraction, analysis, and data reduction can be found in Licht *et al.* (2017). Crystallization age for volcanic samples were calculated using TuffZirc (Ludwig 2003). The final age error calculated for each sample is the quadratic sum of the uncertainty of TuffZirc age calculation and of the systematic uncertainty during each session (~ 1%). Detailed U-Pb data are given in Supplementary Table 1.

4. Description of the measured sections

4.1. Yenipazar section

The Yenipazar Section comprises almost the complete Turonian-Eocene basin-fill and measures 2370 m thick (Figure 4A and SM Figure1). This section starts within the Değirmenözü Formation, an 80 m thick unit formed from the alternation of thin (< 5 cm) pink limestone and red mudstone laminae in the lower part, that is dominated by red mudstones further up-section. Metric slumps are common. Two planktonic foraminifera biozones of late Santonian to early Campanian age, *Dicarinella asymerica* and *Globotruncanita elevata*, are distinguished in the unit (Figures 4 and 5). A gradual colour change to grey and the first appearance of turbidite sandstones mark the transition to the Yenipazar Formation. The Yenipazar Formation consists of alternations of grey mudstone, thin to medium-bedded sandstone and thick to very thick green tuff. Extrabasinal conglomerates up to 5 m thick can sometimes accompany the sandy intervals. Conglomerate clasts (3–5 cm size) are derived from the Lower-Middle Cretaceous limestone and marl, gneiss and ultramafic fragments. Flute casts and asymmetrical ripples from diverse stratigraphical levels indicate palaeocurrents to the NE, NW and less commonly to W. Ignoring siliciclastic intercalations, the total thickness of the tuff levels reaches a maximum of ~ 200 m. In most cases, tuff beds have a basal conglomeratic level with mixed volcanic and siliciclastic gravels. The planktonic foraminifera content of the mudstones is very poor presumably due to frequent volcanism.

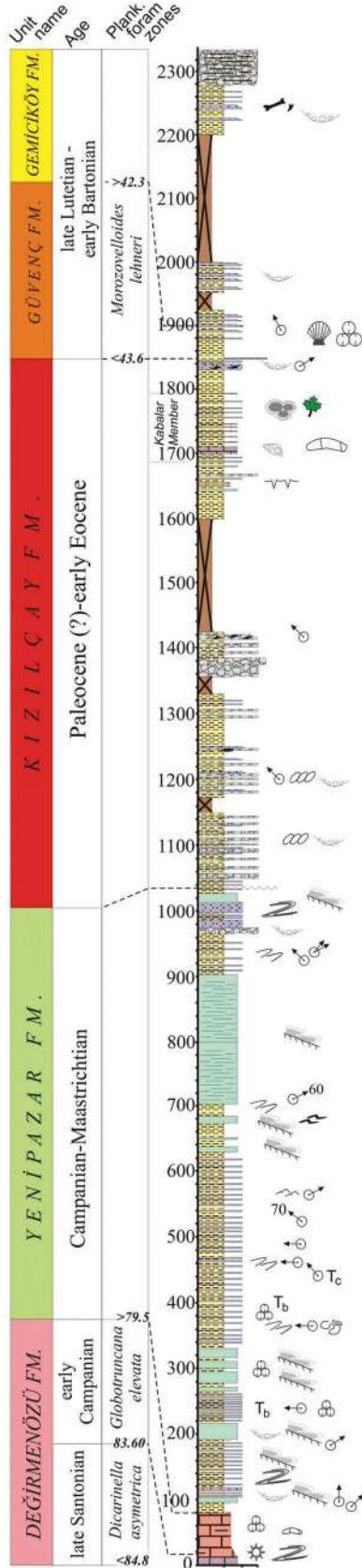
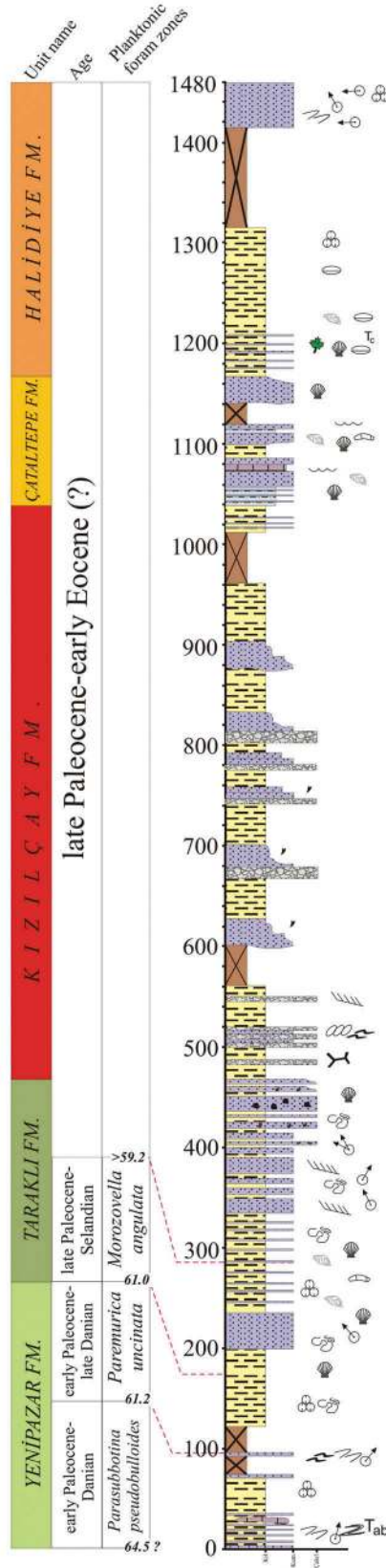
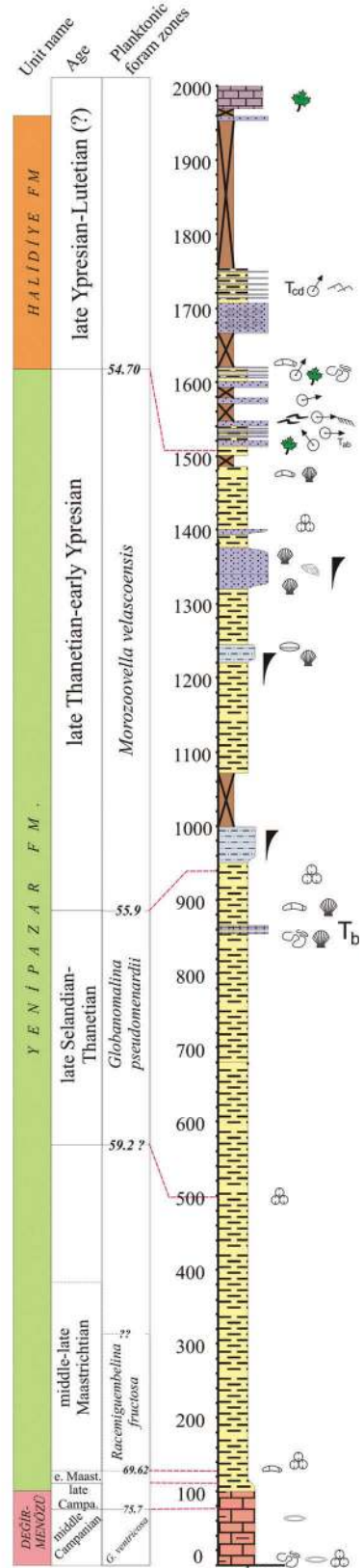
a Yenipazar Section**b** Taraklı Section**c** Akdoğan Section

Figure 4. Detailed sedimentological logs of the Yenipazar (a), Taraklı (b) and Akdoğan (c) Sections including biostratigraphic data (see Figure 2 for location, and Figure 9 for the legend).

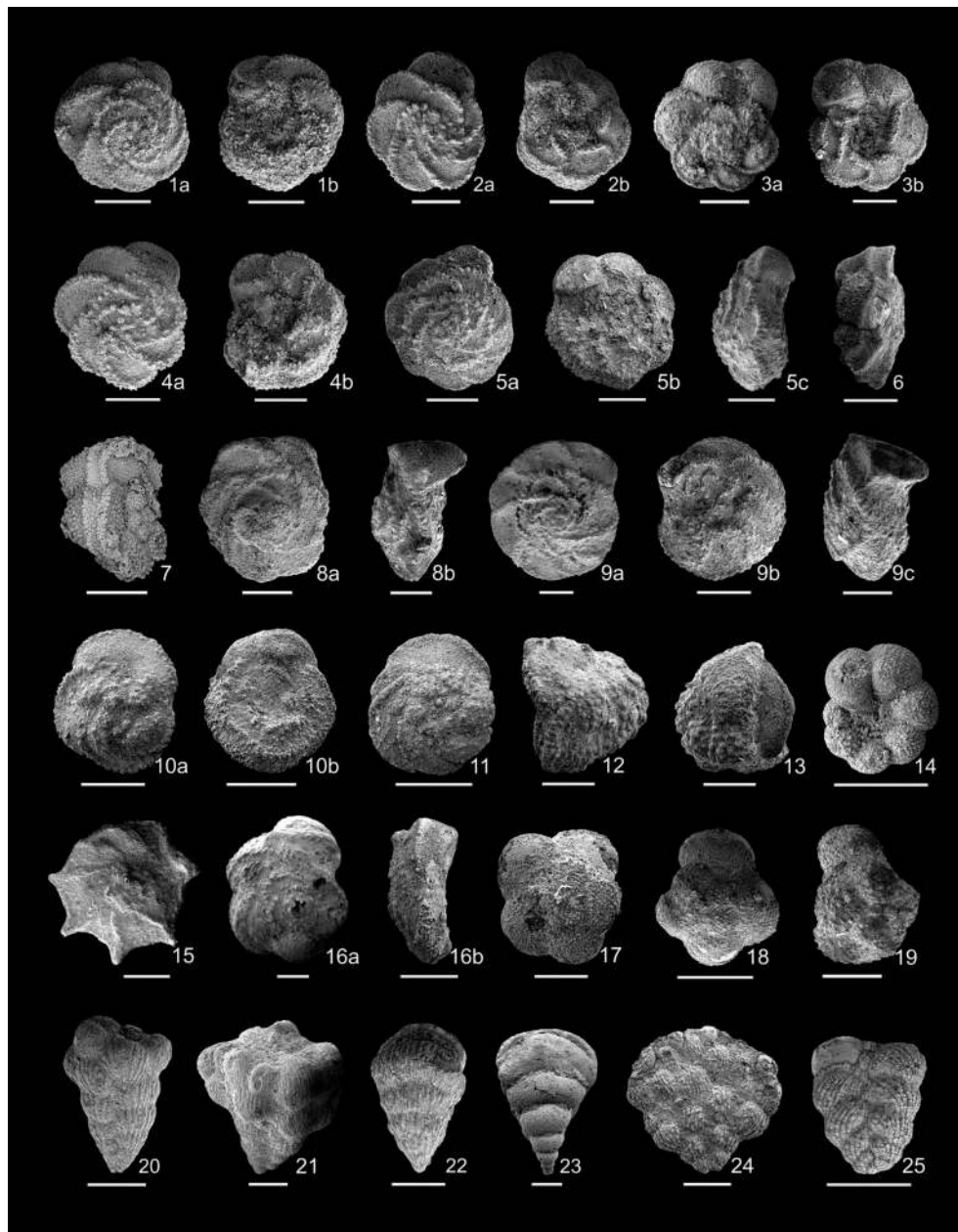


Figure 5. SEM photographs of the upper Santonian-Maastrichtian planktonic foraminifera from the Yenipazar (YP), İsmailler (IS), and Akdoğan (AK) sections, scale bars: 200 μm .

(1) *Marginotruncana coronata* (Bolli), YP-4, a-spiral view, b-umbilical view; (2) *Marginotruncana pseudolinneiana* Pessagno, YP-4, a-spiral view, b-umbilical view; (3) *Marginotruncana marginata* (Reuss), a-spiral view, b-umbilical view, YP-2; (4) *Globotruncana linneiana* (d'Orbigny), YP-3, a-spiral view, b-umbilical view; (5) *Globotruncana arca* (Cushman), IS-22, a-spiral view, b-umbilical view, c-side view; (6) *Globotruncana ventricosa* White, IS-18, side view; (7) *Dicarinella asymetrica* (Sigal), YP-7, oblique view; (8) *Globotruncanita elevata* (Brotzen), IS-3, a-spiral view, b-umbilical view, c-side view; (9) *Globotruncanita stuarti* (de Lapparent), IS-62, a-spiral view, b-umbilical view, c-side view; (10) *Contusotruncana fornicata* (Plummer), IS-62, a-spiral view, b-umbilical view; (11) *Contusotruncana plummerae* (Gandolfi), IS-31, spiral view; (12) *Contusotruncana contusa* (Cushman), IS-69, side view; (13) *Contusotruncana walfischensis* (Todd), IS-69, side view; (14) *Globigerinelloides ultramicrus* (Subbotina), YP-3, peripheral view; (15) *Radotruncana calcarata* (Cushman), IS-16, spiral view; (16) *Abathomphalus mayaroensis* (Bolli), a- IS-77, spiral view, b- IS-85, side view; (17) *Globotruncanella havanensis* (Voorwijk), IS-62, side spiral view; (18) *Globotruncanella petaloidea* (Gandolfi), IS-59, spiral view; (19) *Kuglerina rotundata* (Brönnimann), IS. 42, spiral view (20) *Racemiguembelina powelli* (Smith & Pessagno), IS-77; (21) *Racemiguembelina fructicosa* (Egger), IS-77; (22) *Pseudotextularia elegans* (Rzehak), IS-57; (23) *Pseudotextularia nuttalli* (Voorwijk), IS-74; (24) *Planoglobulina acervulinoides* (Egger), IS-62; (25) *Heterohelix semicostata* Cushman, IS-30.

The Yenipazar Formation is overlain by the Kızılcay Formation along a prominent angular unconformity (Figure 4A). The basal sediments above the

unconformity surface are made from angular boulders and gravels of tuff and marl derived from just beneath. Up-section, the unit is organised by alternating

conglomerates, sandstones and caliche bearing mudstones as well as clayey limestones with an overall thinning-upward trend. Gravel imbrications and channel geometries indicate palaeocurrents towards the NW. In the uppermost part of the Kızılçay Formation, the Kabalar Member is well marked. It is made of a 90 m thick sequence of medium-to-thick bedded mollusca and charophyte bearing limestones, mudstones and bituminous shales. Based on the ostracoda fauna, a Lutetian age is assigned to the unit (Ocakoglu *et al.* 2012). Spectral analysis of the unit pointed out 2.5 m-thick precession cycles (Ocakoglu *et al.* 2012). The Kızılçay Formation is conformably overlain by the mud-dominated shallow marine Güvenç Formation (Figure 4A). This unit consists of medium to thin bedded sandstone-mudstone alternations. Mudstones contain rich planktonic foraminifera fauna along with various bivalvia. This pelagic planktonic foraminifera fauna yields *Acarinina bullbrooki* (Bolli), *Acarinina praetopilensis* (Blow), *Guembeltrioides nuttalli* (Hamilton), *Globigerinatheka subconglobata* (Shutskaya), and *Turborotalia frontosa* (Subbotina), indicating a late Lutetian to early Bartonian age (Figure 6).

The Gemiciköy Formation gradually overlies the Güvenç Formation (Figure 4A). The lowermost 50 m is formed from mudstone and cross-bedded sandstone alternations. Following a coarsening upward trend, maximum clast size of components including gabbro, quartzite, radiolarite, basaltic lava, and lacustrine limestone reaches 25 cm. Large basaltic lava and limestone blocks appear for the first time in the section.

4.2. Taraklı section

The Taraklı Section begins from the hinge of an anticline and extends to the subsequent synclinal axis in the vicinity of Taraklı (Figures 2 and 4B). This 1480 m-thick section comprises several formal units. The basal Yenipazar Formation formed from thin-to-medium bedded sandstone and mudstone alternations, which exhibits occasional slumps and Cretaceous limestone olistolites. Flute casts indicate NNE- and NE-directed palaeocurrents (Figure 4B & SM Figure 2). Planktonic foraminifera biozones of *Parasubbotina pseudobulloides* and *Praemurica uncinata* indicate a late Danian age (~ 61 Ma) for the upper part of the unit. The Taraklı Formation gradually covers the Yenipazar Formation (Figure 4B). This unit comprises the alternation of fossiliferous medium to thick-bedded sandstones and mudstones. Some sandy intervals display large scale cross stratifications. The unit can be further subdivided into two distinct coarsening upward sequences between 180–220 m and 220–480 m. In the lower part of the unit, we distinguished a planktonic foraminifera zone of

Morozovella angulata (early Selandian) (Figure 4B). Large-scale cross bedding and groove casts indicate palaeocurrent directions heading to NW and NE. The Kızılçay Formation gradually overlies the Taraklı sandstones. It starts with sandstone and fine conglomerate alternations, and vertically evolves into thick (4–5 m) alternating conglomerates and thick red/green mudstones. Components of conglomerates are 4–5 cm and are derived from beige Cretaceous limestone, gabbro, radiolarite, and tuff. The Çataltepe Formation is composed of alternating fossiliferous sandstone, limestone, and mudstone, which transgressively overlies the Kızılçay Formation (Figure 4B). In this unit, sandstones are well-sorted and display symmetrical ripples. Thin coal and bituminous-smelling limestones are also present. Although richly fossiliferous, the unit did not yield any planktonic foraminifera. A rich ostracoda fauna including *Cytherella* sp., *Hemiopprideis montoza*, *Neosyprideis* cf., *williamsonia* indicates a probable early Eocene age. A gradual decrease in grain size gives rise to the Halidiye Formation. This unit is formed from the alternation of thick mudstone and turbiditic sandstone. Mudstone intervals are frequently composed of tiny mollusca and bivalvia shells, but are sparse in terms of planktonic foraminifera. Sandstones are thin (< 20 cm, rarely 100 cm), sharp-based and rich in plant debris. Ta and Tb Bouma sequences are the most common sedimentary structures. Asymmetrical ripples and flute casts indicate palaeocurrents from E to W (Figure 4B).

4.3. Akdoğan section

The Akdoğan Section starts close to the metamorphic basement of the CSB and continues until the synclinal axis in the south (Figure 4C and SM Figure 3). The basal Değirmenözü Formation is composed of finely bedded pink mudstone and marl. Planktonic foraminifera, inoceramids, mm-sized bivalvia shells as well as *Zoophycos* trace fossils are abundant in the unit. An apparent gradual decrease in carbonate content and grey colour mark the boundary with the Yenipazar Formation. This unit is dominated by mudstones but includes three massive coarsening upward sandstone sequences (each several tens of metres thick and rich in bivalvia fauna). Very rarely, sharp-based, thin classical turbidite beds can also be found. Three planktonic foraminifera zones (*Racemigumbelina fructifera*, *Globanomalina pseudomenardii*, and *Morozovella velascoensis*) have been distinguished, indicating a late Maastrichtian to early Ypresian age (Figures 4 and 6).

The Yenipazar Formation grades upward to the Halidiye Formation, which consists of turbiditic sandstone-mudstone alternations. Both lithologies are rich in plant debris. Sandstones are sharp-based, medium-

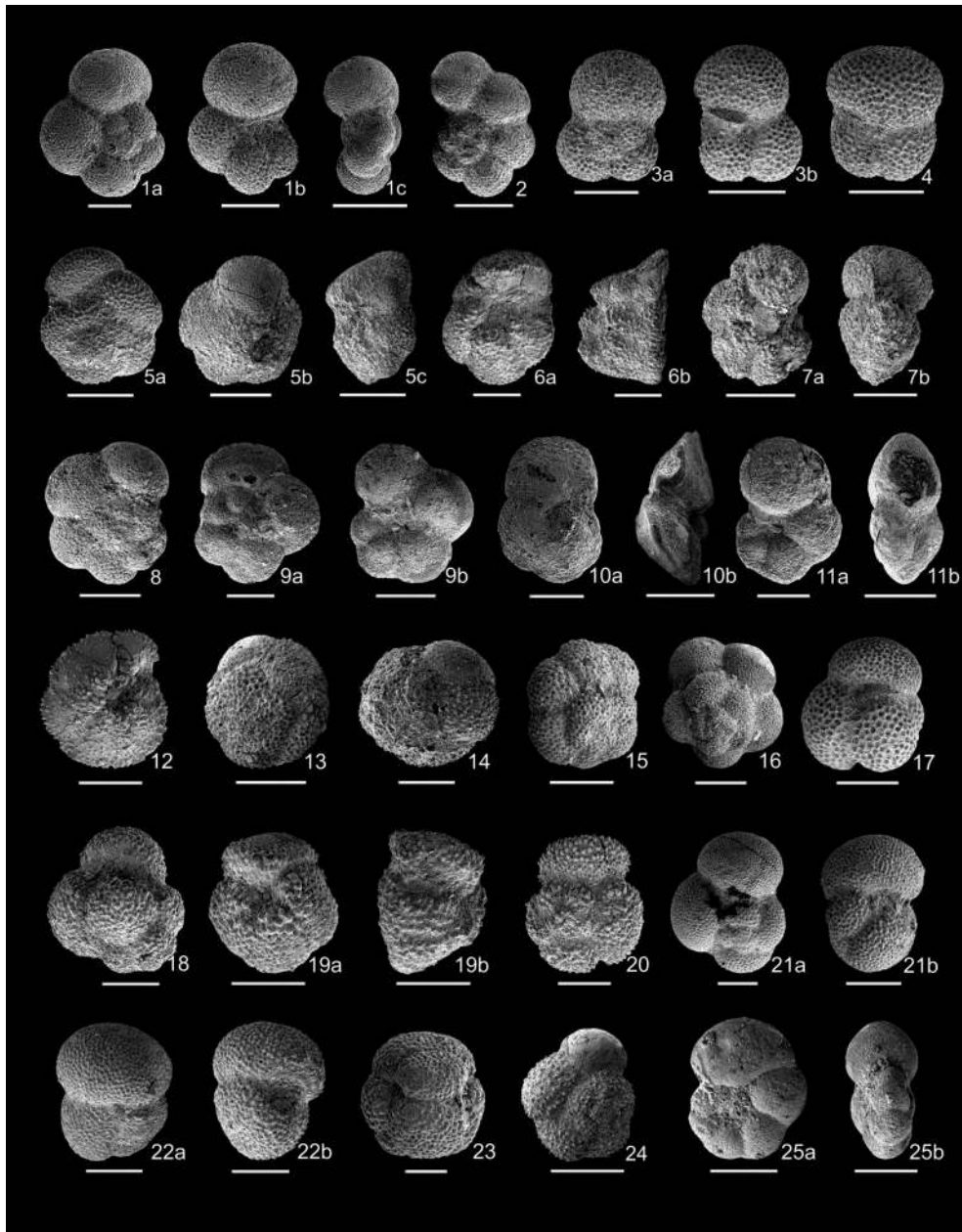


Figure 6. SEM photographs of the Palaeocene and middle Eocene planktonic foraminifera from the İsmailler (IS), Akdoğan (AK), Taraklı (TR), and Yenipazar (YP) sections, scale bars: 150 μ m.

(1) *Parasubbotina pseudobulloides* (Plummer), IS-91, (a) spiral view, (b) umbilical view, (c) side view; (2) *Praemurica pseudoconstans* (Blow), IS-91, spiral view; (3) *Subbotina trilocolinoides* (Plummer), IS-91, (a) spiral view, (b) umbilical view; (4) *Subbotina velascoensis* (Cushman), AK-50, umbilical view; (5) *Morozovella angulata* (White), IS-96, (a) spiral view, (b) umbilical view, (c) side view; (6) *Morozovella conicotruncata* (Subbotina), (a) umbilical view, IS-94, (b) side view, IS-96; (7) *Praemurica uncinata* (Bolli), TR-11, (a) umbilical view, (b) side view; (8) *Praemurica inconstans* (Subbotina), IS-91, spiral view; (9) *Globanomalina ehrenbergi* (Bolli), IS-94, (a) spiral view, (b) umbilical view; (10) *Globanomalina pseudomenardii* (Bolli), (a) spiral view, AK-14, (b) side view, IS-95; 11. *Globanomalina chapmani* (Parr), (a) umbilical view, AK-14, (b) side view, IS-94; (12) *Morozovella occlusa* (Loeblich and Tappan), AK-14, umbilical view; (13) *Acarinina nitida* (Martin), AK-26, spiral view; (14) *Acarinina subsphaerica* (Subbotina), AK-29, side view; (15) *Igorina* sp., YP-128, spiral view; (16) *Eoglobigerina spiralis* (Bolli), IS-91, spiral view; (17) *Subbotina hornibrooki* (Brönnimann), IS-100, spiral view; (18) *Guembelitrioides nuttalli* (Hamilton), YP-128, side view; (19) *Acarinina bullbrooki* (Bolli), YP-128, (a) umbilical view, (b) side view; (20) *Acarinina praetopilensis* (Blow), YP-128, spiral view; (21) *Subbotina eocaena* (Gümbel), YP-130, (a) spiral view, (b) side view; (22) *Turbototalia frontosa* (Subbotina), YP-127, (a) spiral view, (b) side view; (23) *Globigerinatheka subconglobata* (Shutskaya), YP-128, side view; (24) *Acarinina collactea* (Finlay), YP-128, spiral view; (25) *Pseudohastigerina micra* (Cole), YP-128, (a) peripheral view, (b) side view.

to-thin bedded (< 1 m) and are organized as 5- to 10-m-thick lobes. Individual sandstone beds comprise mud-chips, parallel laminations (Tb) and unidirectional ripples (Tc). Groove and flute casts coherently indicate

palaeocurrents moving to NE and NW, and rarely E (Figure 4C). Following a thick covered interval, the section resumes with bluish marl-limestone alternations above the massive, non-fossiliferous sandstones. These

micritic beige limestones with many ostracoda moulds and plant fragments closely resemble to the lithologies encountered in the Kabalar Member in the Yenipazar section.

4.4. Nallihan section

The base of the Nallihan Section starts with the 90-m-thick pink-coloured Değirmenözü Member (Figure 7A and SM Figure 4). This unit consists of the alternation of slumped micritic limestones, marls and mudstones. The unit is rich in nannofossil, inoceramid, ostracoda and bivalvia. Some mudstone intervals also include coalified plant debris.

The overlying Yenipazar Formation consists mostly of grey-to-bluish coloured mudstones and thin turbiditic sandstones. The lower part of the unit comprises two m-thick black shale intervals (Figure 7A). Asymmetrical ripples and flute casts indicate palaeocurrents trending N and NNW. We distinguished the Eymür Member between levels 280 and 410 m in the Yenipazar Formation (Figure 7A), composed of gravelly sandstone, conglomerate and a lesser amount of mudstone. Sandstones comprise cm-thick coalified plant debris. Conglomerates are mostly clast supported and include large (> 3 m) angular boulders of Lower Cretaceous limestones beside medium sized, rounded gneiss and granite pebbles. The interbedded mudstones include rare planktonic foraminifera some of which are reworked from the Middle to Lower Cretaceous.

The red to grey to dark grey marl succession beneath the Eymür Member in this section is of early Campanian age based on the occurrence of the nannofossil marker species *Marthasterites furcatus*, *Broinsonia parca constricta* (CC18b, UC14b-c), *Ceratolithoides verbeekii*, *Lithastrinus grillii* (CC19, UC14d-15a). In the upper part of this section *Ceratolithoides aculeus* has its first occurrence which defines the base of CC20 and UC15b. The ca. 25-m-thick grey shale and marl interval below the first distinctive conglomerate bed of the Eymür Member yields a similar nannofossil assemblage with *Ceratolithoides aculeus* but, in addition, also includes the marker species that defines the next nannofossil zone with its first occurrence (FO), *Uniplanarius sissinghii*. The same assemblages and zonal markers were found in grey shales above the conglomerate unit along the section. This dates the conglomerates of the Eymür Member into the nannofossil zones CC21 and UC15c, respectively, which correspond to the base of the Upper Campanian (Burnett *et al.* 1998) or the upper part of the Middle Campanian of Ogg *et al.* (2012). According to the numerical age calibrations compiled by Anthonissen and Ogg (2012) this correlates to a time

interval from 77.61 Ma (base of *Uniplanarius sissinghii*) to 76.82 Ma (base of *Uniplanarius trifidus*). A biostratigraphic study by Tansel (1980) previously considered the Eymür Member within the *Radotruncana calcarata* Zone. Following ~ 100-m-thick marine mudstones, another sequence of turbiditic mudstone-sandstone alternations (15–20 m thick) is observed. Well-preserved flute casts indicate palaeocurrents towards the NE. Up section, a sandy intertongue within marine mudstones is remarkable at levels 780–800 m. This interval typically coarsens upwards and comprises very large mollusca and echinoderm fossils including *Pycnodonte vesicularis* Lamarck and *Micraster* cf., *cortestudinarium* Goldfuss. Around 1000 m in to the section, planktonic foraminiferal fauna including *Globotruncana arca*, *G. linneiana*, *Rugoglobigerina pennyi*, *Laeviheterohelix glabrans*, *Heterohelix globulosa*, *Globigerinelloides messinae*, *Pseudoguembelina* sp., indicates late Campanian-Maastrichtian age presumably very close to K-Pg boundary. Conformably, the sample at level 1060 m comprises the planktonic foraminifera association that represents the *Guembelitria cretacea-Parasubbotina pseudobulloides* zones of the early Palaeocene (Figure 7A).

A gradual increase in grain size marks the passage to the Taraklı Formation at 1120 m (Figure 7A). This unit is formed from a dozen of massive sandy bodies over the mudstone-siltstone intervals. Sandstones are heavily bioturbated and host a rich mollusca fauna (*Pycnodonte vesicularis* Lamark, *Turritella* sp., *Micraster* cf., *corangium* Klein). The unit itself displays an overall coarsening upward trend, the top of which is formed from 7–8 cm gravel clasts sourced from the Cretaceous carbonates and basement gneiss.

Following the shoaling of the Taraklı Formation, deposition of thin (< 15 cm) coal beds, cross bedded gravelly sandstone and caliche bearing red mudstone mark the onset of deposition of the Kızılçay Formation (Figure 7A). Coarse fluvial clastics include abundant reworked marine microfauna. The successive stratigraphic levels of the Kızılçay Formation are formed from the alternation of clast-supported conglomerate, sandstone and caliche bearing mudstones. Maximum clast size of the unit increases upward to > 25 cm. Clast imbrications and cross-beddings mark palaeocurrents trending NNW and NE (Figure 7A).

4.5. Okçular section

The lowermost part of the Değirmenözü Formation is composed of pink to green mudstone-marl alternations (Figure 7B and SM Figure 5). Three distinct light blue tuff layers (4–10 m thick) also occur in this alternation.

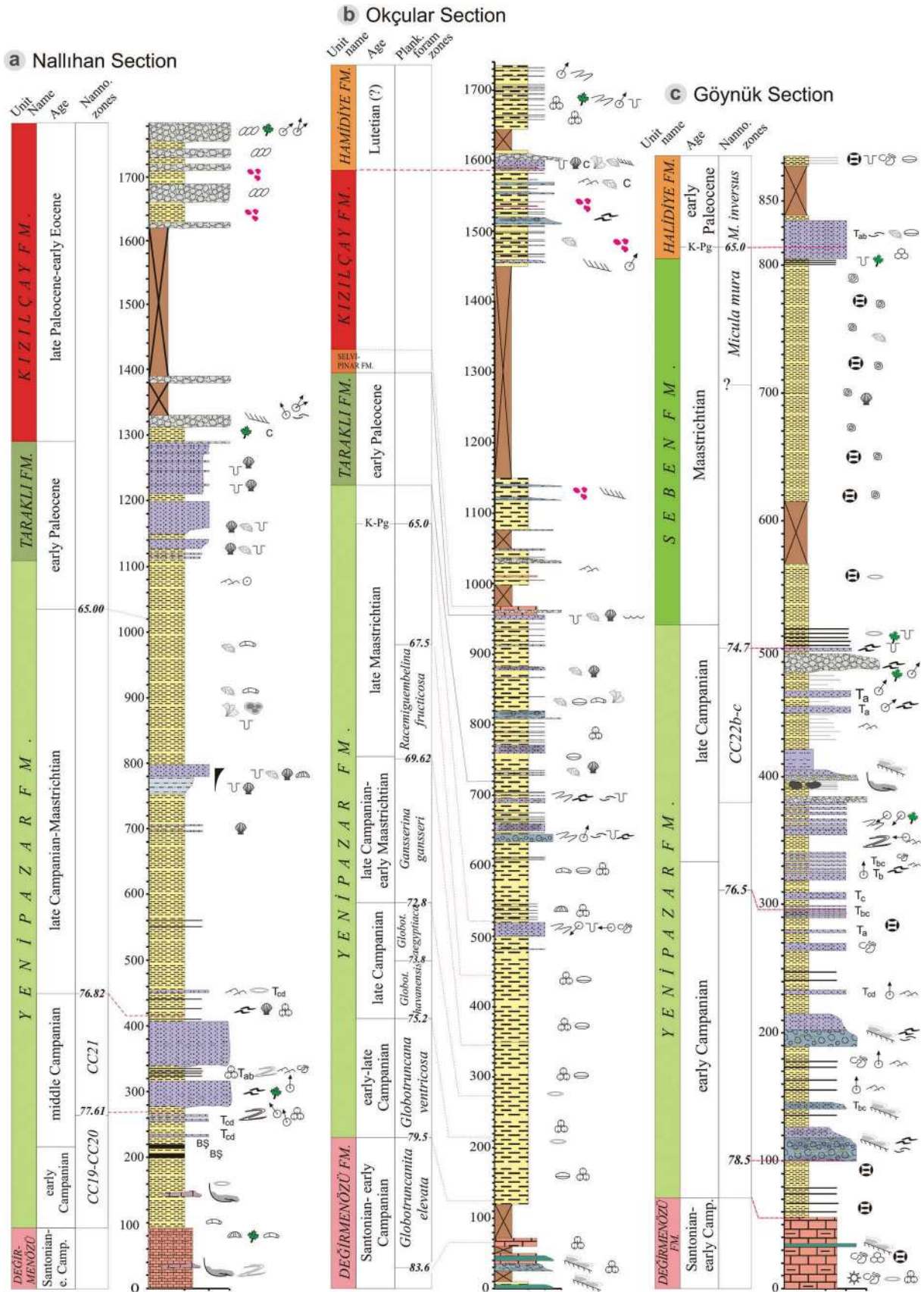


Figure 7. Detailed sedimentological logs of the Nallıhan (A), Okçular (B), and Göynük (C) Sections including biostratigraphic data (see Figure 2 for location, and Figure 9 for the legend).

Tuff layers are finely laminated and contain lapilli-sized quartz and feldspar crystals as well as elongated marl/tuff rip-ups up to 40–50 cm. Just above the tuffs, we identified index fossils *Globotruncanita elevata* indicating an early Campanian age.

The transition to the Yenipazar Formation is gradual and marked by a change to more greyish colours and increase in carbonate content. The basal part of this unit (120–500 m) is entirely composed of mudstone where four planktonic foraminifera zones are distinguished (Figure 7B). Further up-section, turbiditic sandstone-mudstone alternations appear. Previous geochemical and biostratigraphical studies revealed that the K-Pg boundary is situated just above the first turbiditic sandstone sequence (Açıklın *et al.* 2015) (Figure 7B). Individual horizons in this sequence are often thick-bedded (~ 130 cm) and comprise Ta and Tb Bouma sequences, groove and flute casts, all indicating palaeocurrents heading to the W and NNW (Figure 7B). Interbedded mudstones have a rich microfauna of planktonic foraminifera (*Eoglobigerina* spp., *Subbotina* spp.) benthic foraminifera, and ostracoda. The contact between the Yenipazar Formation and the overlying Taraklı Formation is placed over the grey-blue mudstone at 735 m, where the first and abundant mollusca macro-fossils are encountered in this section. The Taraklı Formation is formed from thick mudstone and sandstone alternations. Mudstones include both micro-fossils (*Globigerina* sp., *Subbotina* sp., as planktonic foraminifera and undetermined benthic foraminifera) and macro-fossils (*Ceratotrochus cuisine* (coral), *Cryaca uncifra* and *Barbatia subbarbatula* (bivalvia)) collectively indicating a gross early Palaeocene age. Sandstone beds always include some cross-bedded gravel lenses with abundant macrofossils. The Taraklı Formation is conformably overlain by the Selvipınar Formation, a thin (~ 15 m) unit of dominantly fossiliferous, partly detrital carbonate. The Kızılçay Formation conformably overlies the Selvipınar Formation (Figure 7B). This unit is made from thick (> 10 m) red-to-grey mudstone and thick (4–5 m) channelized conglomerate/sandstone alternations. Mudstone intervals are frequently 30- to 40-cm-thick caliche beds. In two different stratigraphic levels (1484 m and 1572 m), we encountered lacustrine limestones with gastropod shells. Components of conglomerates are well rounded, and are mostly composed of quartzite, gabbro, radiolarite and intraformational mudstones. Widespread planar and trough-cross bedding in overlying sandstones indicate NE-directed palaeocurrents (Figure 7B).

A fining-upward marine sequence (Halidiye Formation) transgressively overlies the terrestrial Kızılçay Formation (Figure 7B). The lower, sandstone-

gravely sandstone alternation in this unit displays a series of diagnostic features (well rounded and sorted clasts, occurrence of coal seams etc.) of a littoral zone, and comprises a rich benthonic fauna including bivalvia, gastropoda, and solitary corals. The overlying 100-m-thick fine-grained interval is composed of thin (< 60 cm) sandstone and mudstone alternations with a planktonic foraminifera fauna (*Morozovella* spp., *Acarinina* spp.,) of poor biostratigraphic significance.

4.6. Göynük section

The Değirmenözü Formation in the Göynük area is up to 170 m thick, of which only the uppermost 55 m is displayed in our section (Figure 7C and SM Figure 6). Thin (5–10 cm) micritic limestone beds alternate with mm-thick red mudstones. Both lithologies include rich fauna of planktonic foraminifera, nannofossils, radiolarians and inoceramids. Radiolarian fauna give a rather wide time span of late Turonian-early Campanian (determined by U.K. Tekin, Hacettepe University). Three yellow tuff layers up to 2 m thick are interleaved in the section. A recent study by Wolfgring *et al.* (2017) indicated that the unit encompasses the Santonian-Campanian transition and mostly spans early Campanian at the uppermost levels with 5.2-m-thick eccentricity cycles (400 ka). Similar to previous sections, passage to the Yenipazar Formation is demarcated by a decrease in carbonate content and a change to greyer colours. This unit is formed from the alternation of thick tuff and siliciclastic intervals (Figure 7C). Three tuff levels at 100 m, 140 m, and 200 m are cumulatively 25 m thick. Each tuff bed is typically sharp-based, thins upward, and comprises dm- to m-sized rip-up clasts and shell fragments in a sand-sized quartz and feldspar background. Groove and flute casts are common. The siliciclastic part of the unit consists of thick grey mudstone and thin (< 15–20 cm) turbidite sandstones. Sandstones frequently display Tb, Tc-d Bouma sequences and unidirectional ripples that indicate palaeocurrents heading to N and NE (Figure 7C). Several thick channelized conglomeratic levels (3–10 m thick) with well-rounded clasts up to 20 cm also interleave with finer clastics. Gravels are mostly derived from radiolarite, beige Lower Cretaceous carbonate and intraformational mudstone and sandstone. Around 390 m in to the section, huge (several ten to hundred m-sized) olistostromes and broken formations are observed in two distinct stratigraphic levels (Figure 8). Out of place bodies belong either to Lower Cretaceous pelagic limestones or newly deposited calcareous mudstones. Slickenlines indicate displacement towards the NNW. Two U-Pb ages from zircons are recovered in the

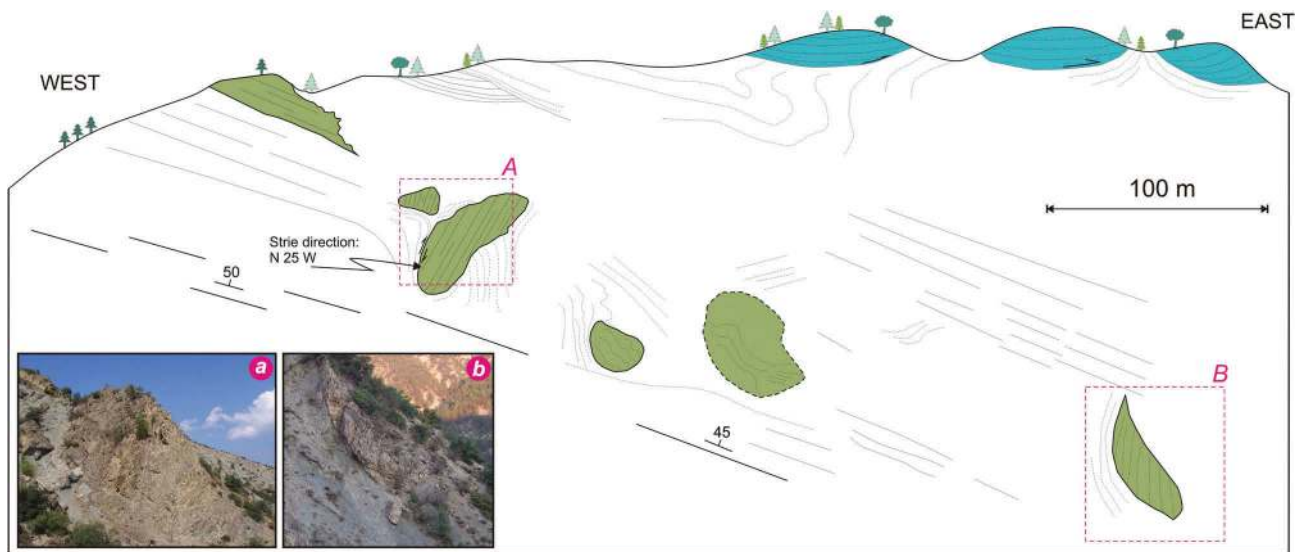


Figure 8. Widespread slumps in the Middle-Late Campanian sediments, 500 m east of the Göynük town. Subfigures display a penecontemporaneous marl block with well-preserved slickensides over the mudstone matrix (A), and a recrystallized Cretaceous limestone block in the shale matrix (B).

unit. The first tuff level at 100 m in this section (Figure 7C) yielded an age of 78.5 ± 1.6 Ma based on $n = 91$ zircons (early Campanian) (Supplementary Table 1). A sandstone bed just beneath the uppermost thick conglomerate at 480 m gives a maximum deposition age of 76.4 ± 1.7 Ma based on $n = 19$ zircons, and established that the majority of zircons are detrital in origin (see Supplementary Table 1).

Samples from grey shale below the conglomerate at level 480 m of the section yield nannofossil assemblages including *Uniplanarius trifidus*, which defines the base of biozones CC22 and UC15d. Other markers such as *Ceratolithoides aculeus* and *Broinsonia parca constricta* are also observed. The absence of *Lithastrinus grillii* (last occurrence of which defines the top of biozone CC22a and the lower part of UC15dTP), the continuous presence of *Eiffellithus eximius* and *Reinhardtites anthophorus*, and the presence of transitional forms from *Reinhardtites anthophorus* to *Reinhardtites levis* (which define the base of CC22c) indicate that this unit belongs to the upper part of biozone CC22 (CC22b-c of Perch-Nielsen 1985) and UC15dTP, below the last occurrence of both *Eiffellithus eximius* and *Reinhardtites anthophorus*. According to these results, the conglomeratic interval at Göynük can be assigned to nannofossil zones CC22b-c and UC15d-eTP, indicating a late Campanian age (Figure 7C).

The Seben Formation gradually overlies the Yenipazar Formation and consists entirely of grey mudstones with abundant nannofossil, bivalvia and gastropoda. Here, the Halidiye Formation is particularly sandy

and gradually overlies the Seben Formation (Figure 7C). This unit is a coarsening upward package of sharp-based sandstone and mudstone alternations. Individual sandstone beds are normally graded and have groove casts and trace fossils including *Ophiomorpha rudis*, *Scoliacia strozzii*, and *Palaeodictyon majus*, all of which indicate deposition in a deep marine environment. The K-Pg boundary is determined to be close to the base of the Halidiye Formation based on the passage from the nannofossil biozone of *Micula murusa* to *Markalius inversus* at the 815 m level of the section (Figure 7C).

4.7. İsmailler section

The İsmailler Section represents the pelagic/hemipelagic deposition in the deeper, northern part of the basin and belongs almost entirely to the Yenipazar Formation except the lowermost and uppermost parts (Figure 9 & SM Figure 7). The Değirmenözü Formation is thicker here and is as old as the Upper Santonian (Yılmaz 2008). Our section begins from the uppermost 30 m of this unit which is composed of alternation of thin (< 10 cm) pink marls and mudstones. Meter-sized slumps are common in the unit. The top of the *Globotruncana elevata* Zone is situated very close to the upper contact of the unit (Figures 5 and 9). The overlying Yenipazar Formation is almost fully composed of mudstones extremely rich in planktonic foraminifera. Eleven planktonic foraminifera zones are distinguished in the unit (Figures 5 & 9). The lowermost part of the Yenipazar Formation comprises a 15-m-thick package of

7 Ismailler Section

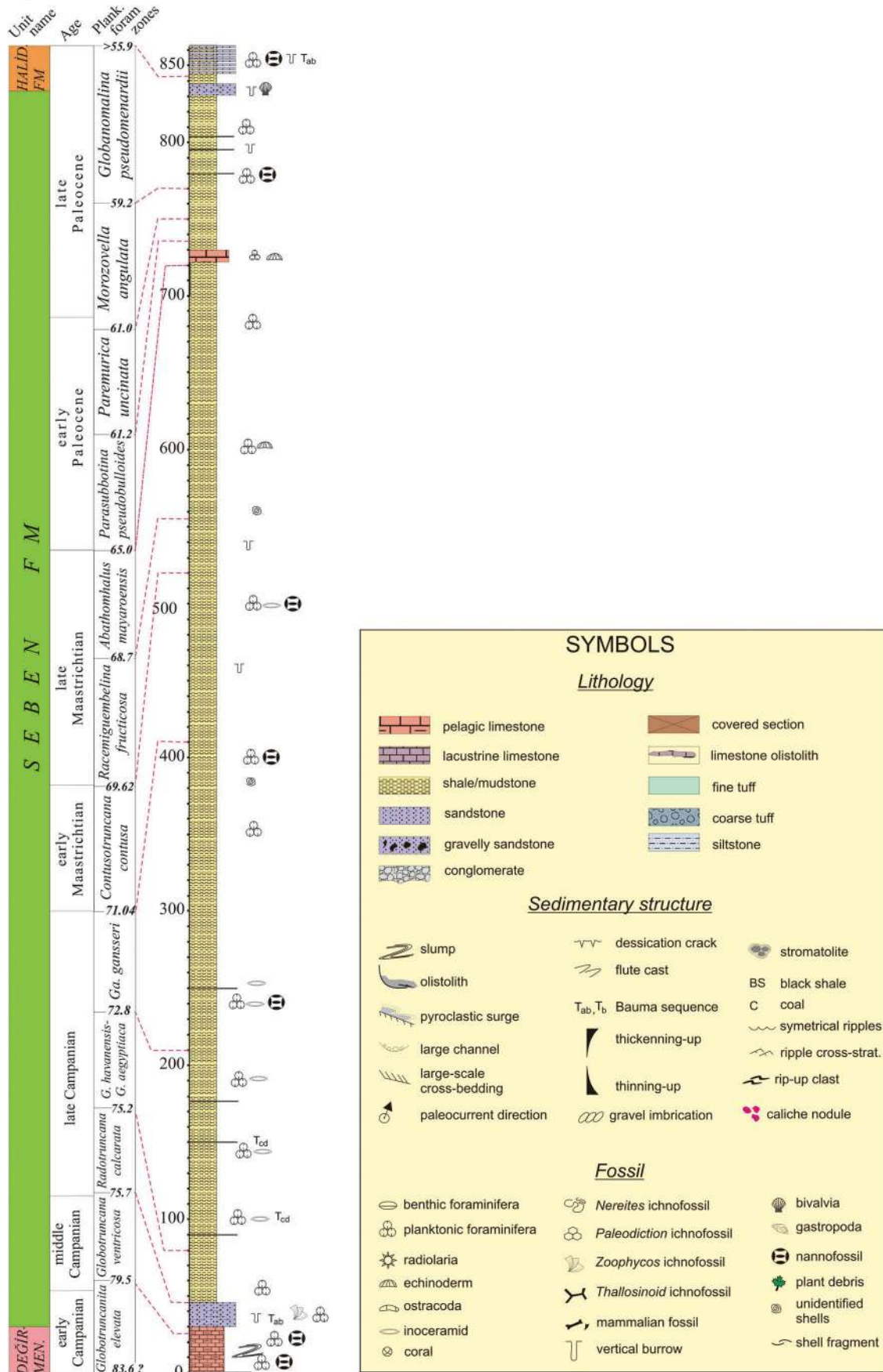


Figure 9. Detailed sedimentological log of the Ismailler Section including biostratigraphic data (see Figure 2 for location).

gradual passages to fine sandstone-marl alternations. Sandstones exhibit parallel laminations and are intensively bioturbated locally by *Echinospira* trace fossils. This sandy interval is entirely restricted to the *Globotruncana ventricosa* Zone (Figure 5). Following a very thick mudstone succession, a carbonate interval is seen just above the K-Pg boundary (Figure 9). This 15 m-thick thin marl-limestone alternations is strikingly similar to the contemporaneous part of the Okçular section 40 km to the SE. Following another thick interval of mudstones, sharp-based medium-to-thick beds of the Halidiye Formation appear at the top of the section. Interbedded mudstones include planktonic foraminifera, nannofossil and ostracoda fossils. The Halidiye Formation is confined to the uppermost part of the *Globanomalina pseudomenardii* Zone (~ 55.9 Ma) (Figures 6 and 9).

5. Basin-fill architecture

Here, the measured sections are assembled in order to build two SE-NW bearing geotraverses on the basis of their geographic positions in the basin (Figures 10 & 11). In order to aid comprehension regarding the timing of sedimentary events, we have also constructed temporal geotraverses (Figure 12) based on the linear extrapolation of the available biozone age data. These nonpalinspastic reconstructions are based on the

correlation of depositional environments in the adjoining sections tied by planktonic foraminifera and nannofossil biozones, as well as U-Pb age data. Numerical ages of planktonic foraminiferal zones are compiled from Robaszynski and Caron (1995), Berggren *et al.* (1995), Berggren and Pearson (2005), Petrizzo *et al.* (2011), Wade *et al.* (2011), Gradstein201616, and Coccioni and Silva (2015). We have also calculated sedimentation rates with time based on the thickness of sediments deposited during the individual planktonic foraminiferal zones in different measured sections (Figure 13).

The Yenipazar geotraverse exhibits a 1 km-thick flyschoidal succession (Yenipazar Formation) beneath an early late Palaeocene (~ 61 Ma) angular unconformity (Figure 10). Absolute ages of planktonic foraminifera zones allow us to calculate an overall relatively low sedimentation rate (2.8 cm/kyr), which prevailed during the early Campanian (83.5–79.6 Ma) in a deep marine pelagic carbonate setting. Evidence for repeated slumps in the Değirmenözü Member and palaeocurrent data indicate that the inner, deep parts of the basin were fed by the erosion/dismantlement of a carbonate system located at the southern margin of the basin. Flyschoidal deposition replaced this environment right at the upper limit of the *Globotruncanita elevata* Zone in mid-Campanian (79.6 Ma). Soon after, products of a submarine explosive volcanism start to alternate with

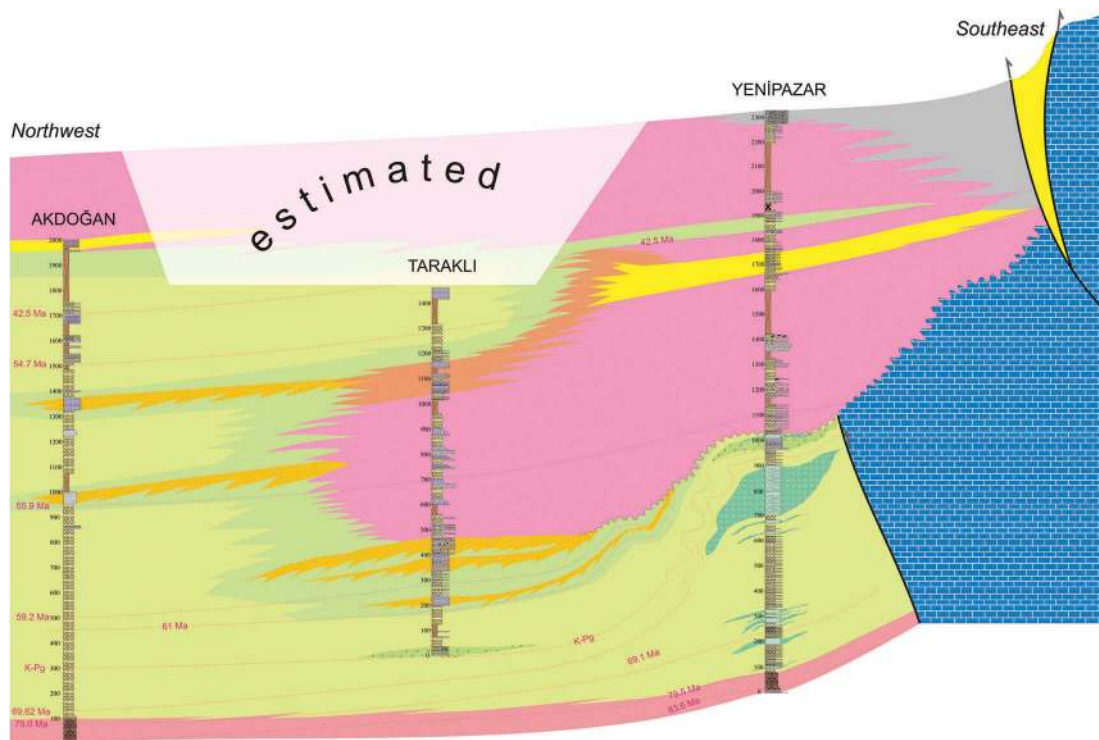


Figure 10. Yenipazar geotraverse (see Figure 2 for the location of the sedimentological logs).

siliciclastic sediments until 900 m in to the section. This huge volume of pyroclastic material may have been sourced from a volcanic centre 10 km west of Yenipazar town, whose subsurface igneous counterparts were mapped by Gedik and Aksay (2002) (Figure 2).

According to the Yenipazar geotraverse, the lateral equivalent of the unconformity surface in the northerly Taraklı section is the 200 m thick sandy Taraklı Formation and not the Kızılcay Formation (Figure 10). The rationale behind this correlation is the gradual passage from basinal sediments to deltaic sandstones of the Taraklı Formation in the northern portions of the basin, compared to direct terrestrial sedimentation on the unconformity surface in the southern areas (Figure 10). Validation of this correlation hinges on being able to date the base of the Kızılcay Formation in the Yenipazar Section – however, internal coherence of the scaled Yenipazar geotraverse strongly suggests that this correlation is correct.

The very base of the deltaic Taraklı Formation starts extremely close to the base of the *Morozovella angulata* biozone (~ 61 Ma) when the sedimentation rate was extremely high (12–42 cm/kyr) (Figure 13). Above the unconformity surface, the Kızılcay Formation occupies the central and northern areas and grades northward to massive mudstones of the Yenipazar Formation. Two progradational delta-front sandy tongues were observed in the Akdoğan section at levels 1000 m and 1350 m, which according to our biozone data likely correspond to the early Thanetian (~ 55.9 Ma) and late Thanetian (~ 55 Ma) respectively.

After these two episodes of deltaic progradation, a marine transgression occurs in Ypresian times (Figure 10). The correlative of this transgression in the southern Yenipazar area is the lagoonal Kabalar Member. Almost contemporaneously, a deep marine turbidite system initiated in the northern Taraklı and Akdoğan sections. Dominant E-W palaeocurrent directions imply an uplifted area north of the basin. The marine Halidiye Formation marks the final, and short-lived transgression in the basin during late Lutetian times reaching as far south as the town of Yenipazar. This major maximum flooding surface of late middle Eocene age can be correlated with other marine units along the suture zone (Licht *et al.* 2017) and potentially corresponds to the 40.4 Ma flooding surface in the global sea level chart of Hardenbol *et al.* (1998). The terrestrial Gemiciköy Formation progradationally overlies marine units and is composed of abundant basaltic lava as well as reworked lagoonal carbonate gravels from the Kabalar Member, indicating the onset of a

basaltic volcanism and on-going tectonic uplift in the south (Figure 10).

The Nallıhan geotraverse displays a similar sedimentary history but omits the last 10 Myr of the Yenipazar geotraverse (Figure 11). In this geotraverse, pelagic carbonate deposition with frequent slumps developed before shifting to flyschoidal deposition at ~ 79.6 Ma. The sedimentation rate during carbonate deposition and just afterward was very low (0.5–0.6 cm/kyr) (Figure 13). A smaller submarine volcano erupted several tuff beds just before the *Globotruncanita elevata* Zone (~ 83.5 Ma) in the Göynük and Okçular section (Figure 11). About 1 Myr following the onset of flysch deposition, another submarine volcano, this time more voluminous, resumed in the Göynük section at ~ 78.7 Ma. After ejecting several very thick tuff intervals in vicinity of Göynük, volcanism ceased around 76 Ma as demonstrated by our younger zircon age and biostratigraphic data from the nearby Karaardıç section (Ocakoglu *et al.* 2007).

The Nallıhan geotraverse also sheds light upon the stratigraphic position of the coarse clastic wedges (Eymür Member) in the Yenipazar Formation (Figure 11). The first siliciclastic wedge is confined within the CC21 nanofossil zone in the Nallıhan section and would be correlated with the Cam 6 major sequence boundary (77.8 Ma) of Hardenbol *et al.* (1998). The second deep marine clastic wedge is recognized and dated to 75.9 Ma in the Göynük section and can be correlated to the Nallıhan section. A third siliciclastic wedge is observed just beneath the K-Pg boundary in the Göynük and Okçular sections (Figure 11) and may be correlated with the Ma5 sequence boundary (65.42 Ma) of Hardenbol *et al.* (1998). The final deep marine siliciclastic wedge is observed in the uppermost part of the İsmailler section around the middle Ypresian (~ 55 Ma) and can also be correlated with Hardenbol *et al.* (1998).

In the late Maastrichtian and early Palaeocene, the Nallıhan area seems to have been in a shelf position as evidenced by the fossiliferous mudstone and deltaic progradation at level 750 m in contrast to the rest of the basin (Figure 11). Deltaic deposition of the Taraklı Formation began on the order of several hundred metres above the K-Pg boundary probably during the late Palaeocene in both the Nallıhan and Okçular sections in agreement with the well-dated Taraklı Section.

The Kızılcay Formation in the Nallıhan geotraverse is about 650 m thick and exhibits a lateral grain size decrease and facies changes from the Nallıhan to

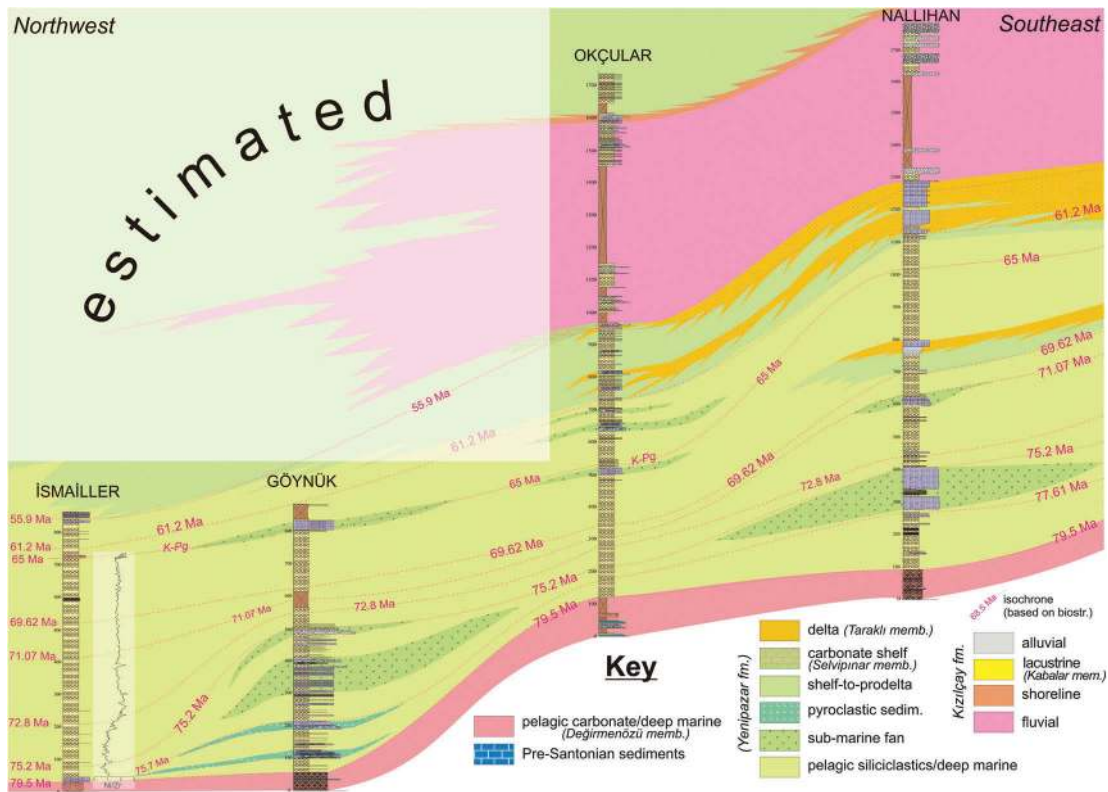


Figure 11. Nallihan geotraverse (see Figure 2 for the location of sedimentological logs).

Okçular sections (Figure 11). The transgressive Çataltepe Formation which is only preserved in the Okçular section is Ypresian (probably latest Ypresian) in age as indicated by macrofossil fauna. The youngest sedimentary record in this geotraverse is the deeper shelf fine sediments of the Güvenç Formation of late Lutetian-early Bartonian age.

6. Discussion

6.1. Tectonic vergence and basin morphology

During the Turonian-early Campanian period, the CSB was dominated by pelagic carbonate deposition (Değirmenözü Member) without significant (if any) sub-areal exposure at its margins that would have sourced siliciclastic influx (Figure 12A, B; Figure 14A). Plurimetric reversed and recumbent slumps observed in the southerly Yenipazar and Nallihan sections seem to have developed on north dipping slopes of the basins southern margin (Figures 10 and 11). Meter-sized olistoliths in the Nallihan section imply active deformation along the southern margin. We thus suggest that during the Turonian-early Campanian times, incipient uplift along the southern margin of the basin was already occurring. It is however only after 79.5 Ma that the siliciclastic influx derived from the uplifted sub-aerially

exposed areas started to choke carbonate deposition, gradually giving rise to siliciclastic sedimentation (Figure 14B). This is well expressed in the rising sedimentation rates in the Okçular and İsmailler sections especially after ~ 76 Ma (Figure 13). At almost the same time, the carbonate deposition in the Haymana Basin, which was developed as an accretionary forearc basin along the southern active margin of the Pontides, was also replaced by siliciclastic deposition, driven by tilting, folding and uplift along the accretionary prism (Okay and Altner 2016).

Our palaeocurrent data from the Yenipazar and Seben Formations show that throughout the Campanian and Maastrichtian, sediment influx was dominantly supplied from the southern margin of the basin, where the accretionary prism of the northward-dipping subduction zone was being built. Somewhat different palaeocurrent directions with a dominant E-W component are attributed to local bathymetric anomalies induced by submarine volcanism. In the İsmailler section, Ocakoğlu *et al.* (2007) and Açıkalın *et al.* (2016) show a significant increase in the elemental rate of Ni/Zr starting at 185 m around ~ 73 Ma (Figure 11). This rise in the Ni/Zr ratio continues for ~ 1.4 Myr until 260 m in to the section, and then remained constant for the rest of the basin-fill. Açıkalın *et al.* (2016) concluded that this increase would correspond to the sub-

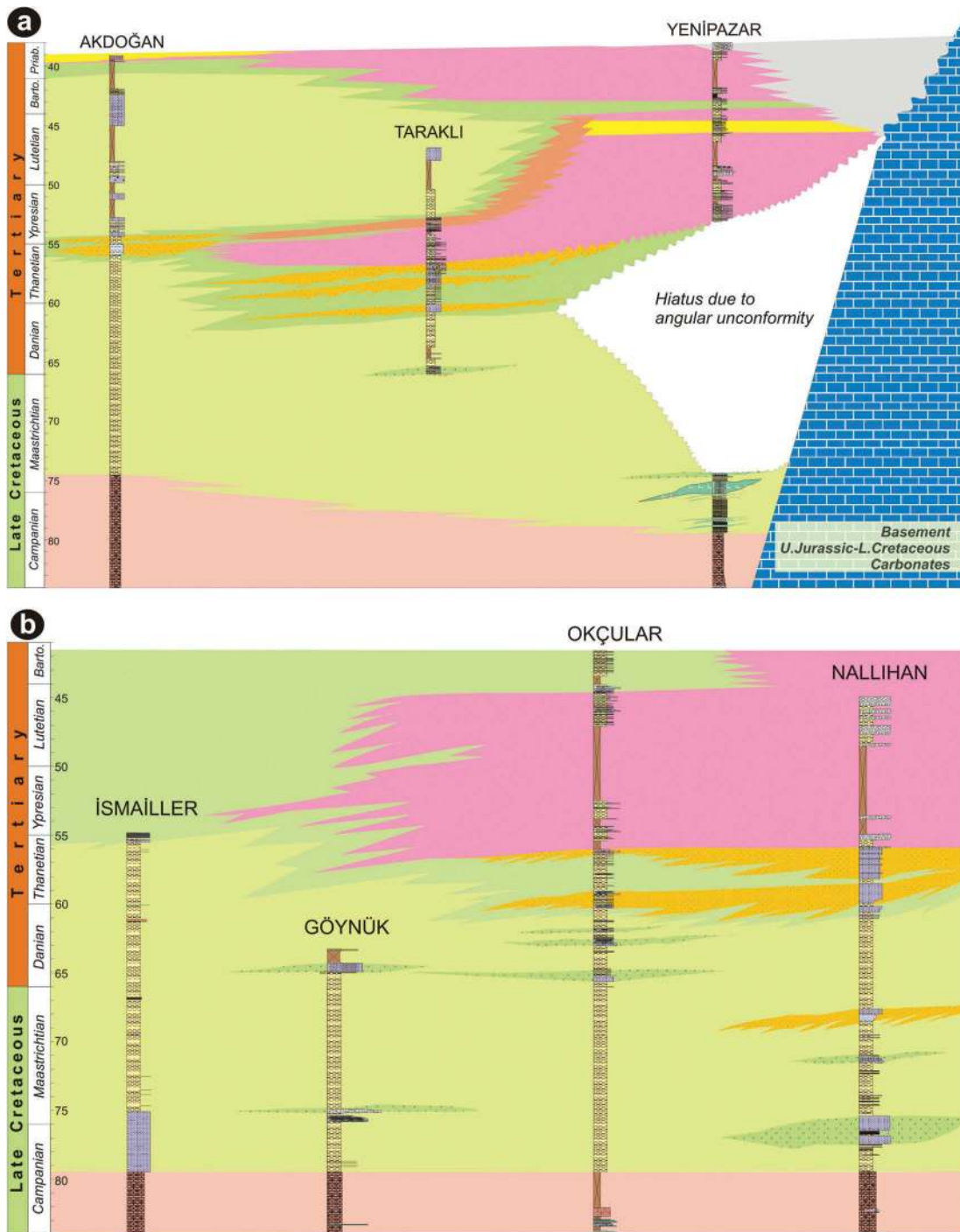


Figure 12. Temporal geotraverses along the Central Sakarya Basin. A- Yenipazar temporal geotraverse B-Nallihan temporal geotraverse.

aerial expansion of subduction-related accretionary prism with ultramafic slices (Figure 14B). During this period, sedimentation rates were extremely high (11–12 cm/kyr) in the İsmailler section (Figure 13). However, it is surprising to see that this anomaly does not match with the major submarine fan development in the Göynük and Nallihan areas (Figure 11).

A massive progradation across the Palaeocene and Eocene was previously suggested in the CSB by Saner 1977, Saner (1980). Both our basin-wide geotraverses refine the suggested timing of events proposed by these early works. Apparent progradation started around ~ 61 Ma over the marine shales and is clearly expressed by the extremely high sedimentation rates

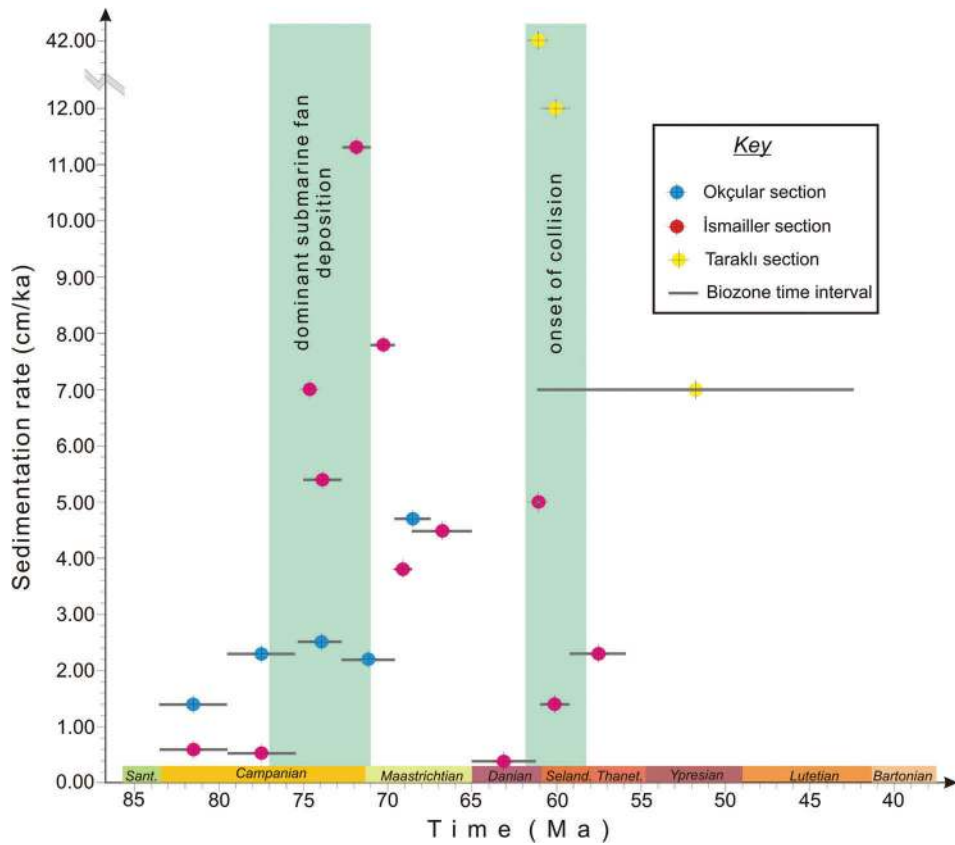


Figure 13. Sedimentation rates with time based on the planktonic foraminifera biozones in three measured sections in the Central Sakarya Basin (see Figure 2 for the location of the sections).

(12–42 cm/kyr) in the Taraklı Section (Figures 12A and 13). During the same period, varying but reduced sedimentation rates were documented in the more basinal İsmailler section, probably due to high frequency relative sea level changes that would have radically shifted the depocentre with time (Figure 13). Sub-aerial depositional environments expanded northward from the accretionary prism to the towns of Taraklı and Göynük in the Thanetian with two exceptional deltaic progradations during the early and late Thanetian (Figure 10, 11, 12A, B & 13C). The last and the most extensive progradation occurred at ~ 47 Ma, shortly after the late Lutetian transgression. Facies and palaeocurrent data indicate an elongated E-W trough between the towns of Taraklı and Akdoğan in the Lutetian. Our palaeogeographic reconstructions match well with the results of Özcan *et al.* (2012) between Kocaeli and the Black Sea coasts in the Pontide Zone, north of our study area. These authors described turbidites in the Santonian-Campanian whilst a volcanic/volcanoclastic succession forms further north. Even if we assume their turbidites as the distal correlatives of the Nallihan-Göynük turbidites, they could also be sourced from

the Campanian magmatic arc situated further north along the Black Sea Mountains.

6.2. Santonian-Campanian arc volcanism

Our results indicate two temporally distinct episodes of volcanism whose products have different thickness and facies intercalated in the Santonian-Campanian sedimentary units. The first is characterized by relatively thin (< 3 m) vitric-to-crystal tuff interbedded within the micritic limestone-mudstone alternations (Ocakoğlu *et al.* 2007). Typical products of this volcanism are encountered only in vicinity of Göynük (Göynük, Okçular and Sünnet sections). In the Okçular section, the position of the tuffs are 20–30 m below the lower limit of *Globotruncanita elevata* Zone (~ 83.5 Ma) and within the *Dicarinella asymetrica* Zone in the Sünnet section. Considering the position of the tuff levels with respect to biozone limits, it seems reasonable to attribute 84.4 Ma for this short-term volcanism.

The second episode of volcanism was more extensive and long-lived compared to the former. Products of this volcanism are composed of grey to green crystal tuffs and found as intercalations in the siliciclastic

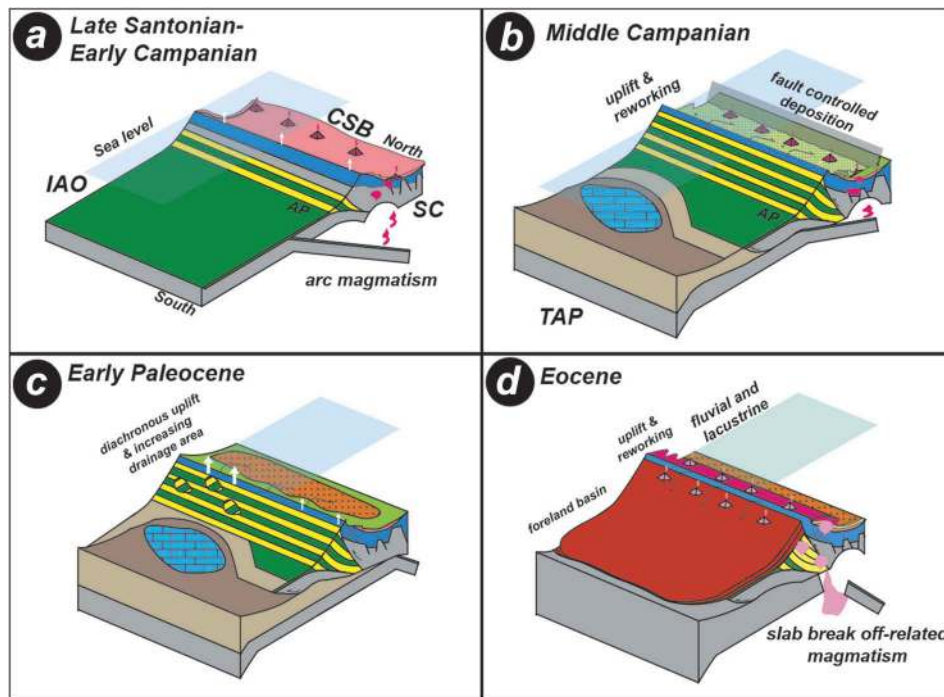


Figure 14. Sketches depicting the plate tectonic evolution of the Central Sakarya Basin across late Santonian-Eocene. (a) Late Santonian-early Campanian: pelagic carbonate sedimentation and coeval arc volcanism related to an intra-oceanic subduction. (b) Middle Campanian: uplift of accretionary prism and onset of turbidite deposition. (c) early Palaeocene: onset of collision, deformation, deltaic progradation, and increased sedimentation rate in the CSB. (d) Late Eocene: Slab tear-related volcanism, progressive deformation in the suture zone and development of a foreland basin (CSB: Central Sakarya Basin, SC: Sakarya Continent, IAO: İzmir-Ankara Ocean, TAP: Tauride-Anatolide Platform, PMS: passive margin sediments).

Yenipazar Formation. As previously suggested, the age of the first tuff by zircon U-Pb dating is ~ 78.5 Ma in the Göynük section. Additionally, in the Karaardıç section (Ocakoğlu *et al.* 2007) the youngest pyroclastic bed occurred very close to the base of the *Globotruncana aegypticata* Zone (~ 74.8 Ma). In this respect, the younger volcanism spans ~ 4 Myr during the middle Campanian. The volcanic products as mapped by Gedik and Aksay (2002) form a grossly E-W belt only 20 km north of the suture belt (Figure 2).

Although the Pontide magmatic arc is commonly considered to be associated with subduction along the İzmir-Ankara and Intra-Pontide suture zones, temporal and spatial refinement of the existing models still need to be achieved. Apart from the volcanic belt recognized here, located in the CSB, another volcanic belt extends across the southern Black Sea shoreline, ~ 80 km north of the study area (Özcan *et al.* 2012). This magmatism is of early Campanian-early Maastrichtian (84–71 Ma) in age and has been shown to be related to subduction (Karacık and Tüysüz 2010). In the Central Pontides further east, another magmatic arc of late Santonian-middle Campanian age is present, which developed at the northern margin of the Sakarya Terrane and is interpreted to be related to south-

vergent Intra-Pontide subduction (Ellero *et al.* 2015). Since many studies suggested that the Intra-Pontide Ocean was already closed prior to the Santonian (see references in Özcan *et al.* 2012), the Santonian-Campanian arc volcanism in the study area should be related to the subduction of the Neotethys along the İzmir-Ankara subduction zone. We suggest that these two distinct arcs could have been created by a roll-back episode along the İzmir-Ankara subduction zone sometime during the Santonian-Campanian times, but further geochronological constrains on the age of volcanism at both localities are needed to confirm this hypothesis.

6.3. An extensional mega-structure in the basin interior?

The map in Figure 2 reveals the E-W trending distribution of the Santonian-Campanian volcanic arc products is grossly sub-parallel to the suture belt in the south. This implies that the volcanic conduits that ejected the voluminous pyroclastics and basaltic lava (Saner 1977, 1980; Göncüoğlu *et al.* 1996) also lined up E-W direction presumably controlled by nearby major faults. The

Olistostromal nature of this volcano-sedimentary unit has been previously documented in the west of the Yenipazar town (Duru *et al.* 2002). Our own observations, shown in Figure 8 demonstrate that the wide-spread slope failure was active in the middle of the basin during the middle-late Campanian. We suggest that some major E-W trending extensional faults enabled the ascent of the magmatic fluids, which formed the Campanian volcanism, and resulted in submarine relief that caused widespread slumping later on. During collision, these faults were likely re-activated as inverted compressional features (Figure 2). Okay and Altiner (2016) have also envisaged extensional tectonics along the forearc in the Haymana basin, located along the southern tip of the Pontide active margin. These authors favoured an extensional intra-arc realm which trapped siliciclastics sourced from the arc, allowing deep marine carbonate deposition to survive until the Campanian in the Haymana Basin. Based on seismic profiles and kinematic data in the Boyabat-Sinop Basin further NE, Hippolyte *et al.* (2015) demonstrated early Cretaceous-Palaeocene extensional structures were structurally inverted during the early Eocene as a result of collision and subsequent indentation.

6.4. Onset of the collision in the Central Sakarya Zone

Here, we show the deltaic Taraklı sandstones began to be deposited in the early Thanetian (~ 61 Ma) in an overall progradational pattern and were sourced from the southern margin of the basin. At the southernmost sites in the basin, near Yenipazar, a contemporaneous angular unconformity developed, suggesting uplift of the southern basin margin (Figure 10, 12A, and 13C). This unconformity is absent near Nallihan, however the first massive deltaic progradation in the Okçular and Nallihan sections is also dated to the early Thanetian (~ 61 Ma). Therefore, the onset of basin-wide deltaic progradation from the south, and uplift in the Yenipazar area indicate a major episode of uplift of the accretionary prism, which we interpret to be related to the onset of collisional tectonics along the Izmir-Ankara Suture. Increased sedimentation rates at this time (Figure 13) substantiate the timing of the onset of collision and the subsequent drainage area widening. The local unconformity near Yenipazar whilst a conformable succession in Nallihan directly to the east can be explained by a protrusion along the suture front.

Previous studies indicated that the Lutetian volcanism (51–47 Ma) at the southern margin of the basin was developed in relation to break-off process of the long-ago subducted oceanic slab (Kasapoğlu *et al.* 2016),

associated with an extensional episode of the overlying upper crust (Okay and Satır 2006; Altunkaynak and Dilek 2013). The findings of the present study do not support an extensional regime in the CSB during the Lutetian. Instead, our data indicate deposition in a retroarc-foreland basin since the late Palaeocene, which received fluvial, lacustrine and shallow marine sediments until the mid-Lutetian (Figure 14D). Appearance of basaltic lava and reworked lacustrine blocks of middle Eocene age within the late Eocene sedimentary rocks reflects further uplift and denudation of the southern margin, as commonly seen in foreland basins. The CSB follows the same foreland basin evolution as the Central Pontide basins (Leren *et al.* 2007; Catanzariti *et al.* 2013; Hippolyte *et al.* 2015). Contemporaneously, a peripheral arc foreland basin to the south began to develop related to the south-directed reverse faults and thrusts, which has yet to be studied in detail (Figure 14D). Deposition in this basin starts directly on the ophiolitic melange and older rocks (Figure 3) (Gedik and Aksay 2002; Yıldız *et al.* 2015) contrary to the continuous sedimentation in the CSB throughout the Cretaceous and Palaeogene.

7. Conclusions

The present study sheds significant light upon convergent margin geodynamics of the Sakarya Terrane, which evolved from subduction to collision during the late Santonian-Eocene, based on a detailed palaeo-environmental and biostratigraphic investigation of the infill of the Central Sakarya Basin.

Our findings indicate that deep marine pelagic carbonate deposition was sporadically accompanied by E-W trending submarine volcanism and underwent significant slumping, probably induced by the already commenced subduction in the south. Uplift and sub-aerial exposure of the accretionary prism related to ongoing subduction triggered deep marine siliciclastic deposition after ~ 79.6 Ma. The widening of the exposed accretionary prism along the southern active margin radically raised sedimentation rates and increased the ultramafic influx to the basin in the latest Campanian (~ 73 Ma). From the middle Campanian to the K-Pg boundary, at least 3 widespread submarine fan systems developed across the southern and central part of the basin. In the late Campanian, widespread slumping involving freshly deposited sediments as well as basement rocks is assumed to be related to a long-lived extensional structure. Throughout the late Campanian-early Palaeocene period, the sedimentation rate continued to rise and reached the maximum values around the Selandian (~ 60 Ma). This time period is

characterized by rapid uplift due to onset of the collision between the Tauride-Anatolide Platform and the Sakarya Terrane in the south, based on a local unconformity and a massive deltaic progradation/terrestrialization across the southern areas of the basin. Our two reconstructed basin fill geotraverses do not display any sedimentary evidence that could witness the occurrence of an active margin in the north throughout the late Santonian-Bartonian period.

Future dating and kinematic studies of the local unconformity in the SW portion of the CSB and the related terrestrial sediments (Kızılcay Formation) will enhance our knowledge about the early collisional processes. Similarly, our suggestion of the long-lived extensional structure in the middle of the basin requires further support by novel kinematic data. Finally the time at which the extensional structure was active must be tuned by more detailed sedimentological and biostratigraphical investigations. These potential data would enrich our existing knowledge on extensional arc/forearc regions.

Highlights

- Campanian-to-Eocene sediments of the Sakarya Terrain is studied for sedimentology and biostratigraphy
- Subduction-related uplift since Early Campanian is documented
- Alignment of volcanic centres and submarine mass movements indicate an extensional forearc realm
- Rapid siliciclastic progradation northward marks onset of collision in Late Danian

Acknowledgments

The authors are grateful to Prof Aral Okay (Istanbul Technical University) and an anonymous reviewer for their comments and suggestions that considerably contributed to the manuscript.

Disclosure statement

No potential conflict of interest was reported by the authors.

Funding

This work was supported by the Scientific and Technological Research Council of Turkey (TÜBİTAK) under Grant 104Y153; National Science Foundation (NSF) under Grant EAR-1543684.

ORCID

Faruk Ocakoğlu  <http://orcid.org/0000-0002-4619-5865>

References

- Açıkalin, S., Ocakoğlu, F., Yılmaz, İ.Ö., Vonhof, H., Hakyemez, A., and Smit, J., 2016, Stable isotopes and geochemistry of a Campanian–Maastrichtian pelagic succession, Mudurnu–Göynük Basin, NW Turkey: Implications for palaeoceanography, palaeoclimate and sea-level fluctuation: *Palaeogeography, Palaeoclimatology, Palaeoecology*, 441, 453–466. DOI:10.1016/j.palaeo.2015.10.005.
- Açıkalin, S., Vellekoop, J., Ocakoğlu, F., Yılmaz, İ.Ö., Smit, J., Özkan-Altiner, S., Goderis, S., Vonhof, H., Speijer, R.P., Woelders, L., Fornaciari, E., and Brinkhuis, H., 2015, Geochemical and palaeontological characterization of a new K-Pg Boundary locality from the Northern branch of the Neo-Tethys: Mudurnu–Göynük Basin, NW Turkey: *Cretaceous Research*, 52, 251–267.
- Akbayram, K., Şengör, A.C., and Özcan, E., 2016, The evolution of the Intra-Pontide suture: implications of the discovery of Late Cretaceous–Early Tertiary melanges: *Geological Society of America Special Papers*, 525, SPE525–18.
- Altiner, D., Koçyiğit, A., Farinacci, A., Nicosia, U., and Conti, M. A., 1991, Jurassic-Lower Cretaceous stratigraphy and palaeogeographic evolution of the southern part of North-western Anatolia: *Geologica Rom*, 27, 13–80.
- Altınlı, İ.E., 1976, Geology of the northern portion of the Middle Sakarya River: İstanbul Üniversitesi Fen Fakültesi Mecm: Seri B, 411–4, 35–56. in Turkish with English abstract
- Altunkaynak, Ş., and Dilek, Y., 2013, Eocene mafic volcanism in northern Anatolia: Its causes and mantle sources in the absence of active subduction: *International Geology Review*, 5513, 1641–1659. DOI:10.1080/00206814.2013.792497.
- Anthonissen, D.E., and Ogg, J.G., 2012, Cenozoic and Cretaceous biochronology of planktonic foraminifera and calcareous nanofossils, in Gradstein, F.M., Ogg, J.G., Schmitz, M.D., and Ogg, G. M., eds., *The geologic time scale*, Elsevier, 1083–1127.
- Berggren, W.A., Kent, D.V., Swisher, I.I.I., C.C., and Aubry, M.P., 1995, A revised Cenozoic geochronology and chronostratigraphy, in Berggren, W.A., ed., *Geochronology Time Scales and Global Stratigraphic Correlation*, SEPM Special Publication No. 54, p. 129–212.
- Berggren, W.A., and Pearson, P.N., 2005, A revised tropical to subtropical Paleogene planktonic foraminiferal zonation: *The Journal of Foraminiferal Research*, 354, 279–298. DOI:10.2113/35.4.279.
- Besbelli, B., 1991, Adapazarı H25 b1,b4,c1 Paftalarının Jeoloji ve Petrol Olanakları. MTA Genel Müdürlüğü, Report No:9237, p. 54 [in Turkish].
- Burnett, J.A., Gallagher, L.T., and Hampton, M.J., 1998, Upper cretaceous, in: Bown P.R., ed., *Calcareous Nannofossil Biostratigraphy*. British Micropalaeontological Society Series, Chapman & Hall/Kluwer Academic Publishing, 132–199.
- Catanzariti, R., Ellero, A., Göncüoğlu, M.C., Marroni, M., Ottria, G., and Pandolfi, L., 2013, The Taraklı Flysch in the Boyalı area (Sakarya Terrane, northern Turkey): Implications for the tectonic history of the IntraPontide suture zone: *Comptes Rendus Geoscience*, 34511–12, 454–461. DOI:10.1016/j.crte.2013.11.001.

- Channell, J.E.T., Tüysüz, O., Bektas, O., and Sengör, A.M.C., 1996, Jurassic-Cretaceous paleomagnetism and paleogeography of the Pontides (Turkey): *Tectonics*, 151, 201–212. DOI:10.1029/95TC02290.
- Çinku, M.C., Hisarlı, Z.M., Heller, F., Orbay, N., and Ustaömer, T., 2011, Middle Eocene paleomagnetic data from the eastern Sakarya Zone and the central Pontides: Implications for the tectonic evolution of north central Anatolia: *Tectonics*, 301, 1–19. DOI:10.1029/2010TC002705.
- Coccioni, R., and Silva, I.P., 2015, Revised Upper Albian–Maastrichtian planktonic foraminiferal biostratigraphy and magneto-stratigraphy of the classical Tethyan Gubbio section (Italy): *Newsletters on Stratigraphy*, 481, 47–90. DOI:10.1127/nos/2015/0055.
- Demirkol, C., 1977, Üzümlü-Tuzaklı (Bilecik) dolayının jeolojisi: *Türkiye Jeoloji Kurumu Bülteni*, 20, 9–16. in Turkish with English abstract
- Duru, M., Gedik, İ., and Aksay, A., 2002, 1/100.000 Ölçekli Türkiye Jeoloji Haritaları. *Adapazarı- H24* Paftası İzahnamesi, Maden Tetkik Arama Genel Müdürlüğü Jeoloji Etütleri Dairesi, Ankara, 34, in Turkish with English abstract
- Ellero, A., Ottria, G., Sayit, K., Catanzariti, R., Frassi, C., Göncüoğlu, M.C., Marroni, M., and Pandolfi, L., 2015, Geological and geochemical evidence for a Late Cretaceous continental arc in the central Pontides, northern Turkey: *Ophioliti*, 402, 73–90.
- Eroskay, S.O., 1965, Paşalar Boğazı–Gölpazarı Sahasının jeolojisi. *İstanbul Üniversitesi Fen Fakültesi Mecmuası*, Seri: B, 30, 3–4, 135–170 [in Turkish].
- Gedik, İ., and Aksay, A., 2002, 1/100.000 Ölçekli Türkiye Jeoloji Haritaları. *Adapazarı-H25* Paftası İzahnamesi, Maden Tetkik Arama Genel Müdürlüğü Jeoloji Etütleri Dairesi, Ankara, 34, in Turkish with English abstract
- Genç, Ş.C., and Tüysüz, O., 2010, Tectonic setting of the Jurassic bimodal magmatism in the Sakarya Zone (Central and Western Pontides), Northern Turkey: A geochemical and isotopic approach: *Lithos*, 1181, 95–111. DOI:10.1016/j.lithos.2010.03.017.
- Göncüoğlu, C., Turhan, N., Şentürk, K., Uysal, S., Özcan, A., and Işık, A., 1996, Geological characteristics of the structural units in Central Sakarya between Nallıhan and Sarıcakaya. *Mineral Research and Exploration Institute of Turkey (MTA) Report*, No. 10094 [in Turkish].
- Göncüoğlu, M.C., Marroni, M., Pandolfi, L., Ellero, A., Ottria, G., Catanzariti, R., Tekin, U.K., and Sayit, K., 2014, The Arkot Dağ Mélange in Araç area, central Turkey: Evidence of its origin within the geodynamic evolution of the Intra-Pontide suture zone: *Journal of Asian Earth Sciences*, 85, 117–139. DOI:10.1016/j.jseaes.2014.01.013.
- Göncüoğlu, M.C., Sayit, K., and Tekin, U.K., 2010, Oceanization of the northern Neotethys: Geochemical evidence from ophiolitic melange basalts within the Izmir–Ankara suture belt, NW Turkey: *Lithos*, 1161, 175–187. DOI:10.1016/j.lithos.2010.01.007.
- Göncüoğlu, M.C., Turhan, N., Şentürk, K., Özcan, A., Uysal, Ş., and Yaliniz, M.K., 2000, A geotraverse across northwestern Turkey: Tectonic units of the Central Sakarya region and their tectonic evolution: *Geological Society, London, Special Publications*, 1731, 139–161. DOI:10.1144/GSL.SP.2000.173.01.06.
- Gradstein, F.M., 2016, Geologic Time Scale, in Harff J., Meschede M., Petersen S., Thiede J., eds., *Encyclopedia of Marine Geosciences. Encyclopedia of Series Earth Sciences*. Springer, Dordrecht, doi:https://doi.org/10.1007/978-94-007-6238-1.
- Granit, Y., and Tintant, H., 1960, Observation préliminaires sur le Jurassique de la région de Bilecik, *CR Acad. Science*, 251: 1801–1803 [in Turkish].
- Hardenbol, J.A.N., Thierry, J., Farley, M.B., Jacquin, T., De Graciansky, P.C., and Vail, P.R., 1998, Mesozoic and Cenozoic Sequence Chronostratigraphic Framework of European Basins, in Graciansky, P.C., et al., eds., *Mesozoic and Cenozoic Sequence Stratigraphy of European Basins*, SEPM Special Publication 60, Tulsa, Charts 1–8, 3–13.
- Hippolyte, J.C., Espurt, N., Kaymakci, N., Sangu, E., and Müller, C., 2015, Cross-sectional anatomy and geodynamic evolution of the Central Pontide orogenic belt (northern Turkey). *International Journal of Earth Sciences: Geologische Rundschau*, 1051, 81.
- Hippolyte, J.C., Müller, C., Kaymakci, N., and Sangu, E., 2010, Dating of the Black Sea Basin: New nannoplankton ages from its inverted margin in the Central Pontides (Turkey): *Geological Society, London, Special Publications*, 3401, 113–136. DOI:10.1144/SP340.7.
- Karacık, Z., and Tüysüz, O., 2010, Petrogenesis of the Late Cretaceous Demirköy Igneous Complex in the NW Turkey: Implications for magma genesis in the Strandja Zone: *Lithos*, 1143, 369–384. DOI:10.1016/j.lithos.2009.09.012.
- Kasapoğlu, B., Ersoy, Y.E., Uysal, İ., Palmer, M.R., Zack, T., Korlay, E.O., and Karlsson, A., 2016, The petrology of Paleogene volcanism in the Central Sakarya, Nallıhan Region: Implications for the initiation and evolution of post-collisional, slab break-off-related magmatic activity: *Lithos*, 246p, 81–98. DOI:10.1016/j.lithos.2015.12.024.
- Kazancı, N., 1979, Haramköy konglomeralarının sedimenter özellikleri (Nallıhan KD/Ankara): *Türkiye Jeoloji Kurumu*, 22, 69–76.
- Koçyiğit, A., Altın, D., Farinacci, A., Nicosia, U., and Conti, A., 1991, Late Triassic – Aptian Evolution of The Sakarya Divergent Margin: Implications For The Opening History of The Northern Neo-Tethys, In *Northwestern Anatolia, Turkey: Geologica Rom*, 27, 13–80.
- Leren, B.L., Janbu, N.E., Nemeč, W., Kirman, E., and Ilgar, A., 2007, Late Cretaceous to early Eocene sedimentation in the Sinop–Boyabat basin, north-central Turkey: A deep-water turbiditic system evolving into littoral carbonate platform, in *Sedimentary Processes, Environments and Basins: A Tribute to Peter Friend*. Nichols, G., Paola, C., and Williams, E.A., eds., IAS Special Publication 38, p. 401–456.
- Licht, A., Coster, P., Ocakoğlu, F., Campbell, C., Métais, G., Mulch, A., Taylor, M., and Beard, K.C., 2017, Tectono-stratigraphy of the Orhaniye Basin, Turkey: Implications for collision chronology and Paleogene biogeography of central Anatolia: *Journal of Asian Earth Sciences*, 143, 45–58. DOI:10.1016/j.jseaes.2017.03.033.
- Ludwig, K.R., 2003, User's manual for Isoplot 3.00: A geochronological toolkit for Microsoft Excel (No. 4). *Berkeley Geochronology Center, Special Publication No. 4*, 74 pp.
- Meijers, M.J., Kaymakci, N., Van Hinsbergen, D.J., Langereis, C. G., Stephenson, R.A., and Hippolyte, J.C., 2010, Late Cretaceous to Paleocene oroclinal bending in the central

- Pontides (Turkey): *Tectonics*, 294, 1–21. DOI:10.1029/2009TC002620.
- Nairn, S.P., Robertson, A.H., Ünlügenç, U.C., Tasli, K., and İnan, N., 2013, Tectonostratigraphic evolution of the Upper Cretaceous–Cenozoic central Anatolian basins: An integrated study of diachronous ocean basin closure and continental collision: Geological Society, London, Special Publications, 3721, 343–384. DOI:10.1144/SP372.9.
- Ocakoğlu, F., 1995, Orhaniye–Güvenç (KB Ankara) karasal çökellerinin Paleosen–Erken Eosen sedimanter evrimi: *Geological Bulletin of Turkey*, 382, 53–66.
- Ocakoğlu, F., and Açıkalın, S., 2009, Paleoclimatic and Source Area Investigation of the Cretaceous–Tertiary Deposits of the Central Sakarya Region, Eskişehir Osmangazi University Research Project no: 200715024, Commission for the Scientific Researches, Eskişehir, Turkey
- Ocakoğlu, F., Açıkalın, S., and Yılmaz, İ.Ö., 2009, A sequence stratigraphic approach to the Mid-Campanian submarine fan development in the Mudurnu–Göynük Basin, NW Anatolia, 8th International Symposium on the Cretaceous System, University of Plymouth, UK, Abstract Book, p. 148.
- Ocakoğlu, F., Açıkalın, S., Yılmaz, İ.Ö., Şafak, Ü., and Gökçeoğlu, C., 2012, Evidence of orbital forcing in lake-level fluctuations in the Middle Eocene oil shale-bearing lacustrine successions in the Mudurnu–Göynük Basin, NW Anatolia: *Journal of Asian Earth Sciences*, 56p, 54–71. DOI:10.1016/j.jseas.2012.04.021.
- Ocakoğlu, F., Yılmaz, İ.Ö., Demircan, H., Altiner, Ö.S., Hakyemez, A., İslamoğlu, Y., ... Szulc, A., 2007, Orta Sakarya Bölgesi Geç Kretase–Paleojen Çökellerinin Sekans Stratigrafisi. The Scientific and Technological Research Council of Turkey (TUBİTAK, Project no: 104Y153), Final Report (450 pp. [in Turkish with English abstract].
- Ocakoğlu, F., Yılmaz, İ.Ö., and Özkan-Altiner, S., 2013, Mid-Campanian Submarine Fan Development in the Mudurnu–Göynük Basin (NW Anatolia): A Sequence Stratigraphic Framework. 9th International Symposium on the Cretaceous System, METU, Ankara, Abstract Book, 81–82,
- Ogg, J.G., Hinnov, L.A., and Huang, C., 2012, Cretaceous, in Gradstein, F.M., Ogg, J.G., Schmitz, M.D., and Ogg, G.M., eds., *The geologic time scale*, p. 793–853.
- Okay, A., and Satır, M., 2006, Geochronology of Eocene plutonism and metamorphism in northwest: *Geodinamica Acta*, 195, 251–266. DOI:10.3166/ga.19.251-266.
- Okay, A.I., 1984, Distribution and characteristics of the north-west Turkish blueschists: Geological Society, London, Special Publications, 171, 455–466. DOI:10.1144/GSL.SP.1984.017.01.33.
- Okay, A.I., 2008, *Geology of Turkey: A synopsis*: *Anschnitt*, 21, 19–42.
- Okay, A.I., Harris, N.B., and Kelley, S.P., 1998, Exhumation of blueschists along a Tethyan suture in northwest Turkey: *Tectonophysics*, 2853, 275–299. DOI:10.1016/S0040-1951(97)00275-8.
- Okay, A.I., Sunal, G., Sherlock, S., Altiner, D., Tüysüz, O., Kylander-Clark, A.R., and Aygül, M., 2013, Early Cretaceous sedimentation and orogeny on the active margin of Eurasia: Southern Central Pontides, Turkey: *Tectonics*, 325, 1247–1271. DOI:10.1002/tect.20077.
- Okay, A.I., Tansel, İ., and Tüysüz, O., 2001, Obduction, subduction and collision as reflected in the Upper Cretaceous–Lower Eocene sedimentary record of western Turkey: *Geological Magazine*, 1382, 117–142. DOI:10.1017/S0016756801005088.
- Okay, A.I., and Tüysüz, O., 1999, Tethyan sutures of northern Turkey: Geological Society, London, Special Publications, 1561, 475–515. DOI:10.1144/GSL.SP.1999.156.01.22.
- Önal, M., Helvacı, C., İnci, U., Yağmurlu, F., Meriç, E., and İzver, T., 1988, Çayırhan kuzeybatı Ankara kuzeyindeki Soğukçam kireçtaşı, Nardin formasyonu ve Kızılçay grubunun stratigrafisi, yaşı, fasiyesi ve depolanma ortamları: *TPJD Bülteni*, 12, 153–163.
- Ottria, G., Pandolfi, L., Catanzariti, R., Da Prato, S., Ellero, A., Frassi, C., Göncüoğlu, M.C., Marroni, M., Ruffini, L., and Sayit, K., 2017, Evolution of an early Eocene pull-apart basin in the Central Pontides (Northern Turkey): New insights into the origin of the North Anatolian Shear Zone: *Terra Nova*, 296, 392–400. DOI:10.1111/ter.2017.29.issue-6.
- Özcan, Z., Okay, A., Özcan, E., Hakyemez, A., and Özkan-Altiner, S., 2012, Late Cretaceous–Eocene geological evolution of the Pontides based on new stratigraphic and palaeontologic data between the Black Sea coast and Bursa (NW Turkey): *Turkish Journal of Earth Sciences*, 216, 933–960.
- Petritzio, M.R., Falzoni, F., and Silva, I.P., 2011, Identification of the base of the lower-to-middle Campanian Globotruncana ventricosa Zone: Comments on reliability and global correlations: *Cretaceous Research*, 323, 387–405. DOI:10.1016/j.cretres.2011.01.010.
- Robaszynski, F., and Caron, M., 1995, Foraminifères planctoniques du Crétacé; commentaire de la zonation Europe-Méditerranée: *Bulletin De La Société Géologique De France*, 1666, 681–692.
- Robertson, A.H., and Ustaömer, T., 2004, Tectonic evolution of the Intra-Pontide suture zone in the Armutlu Peninsula, NW Turkey: *Tectonophysics*, 3811, 175–209. DOI:10.1016/j.tecto.2002.06.002.
- Saner, S., 1977, Geyve – Osmaneli – Gölpazarı – Taraklı Alanının Jeolojisi; Eski Çökeltme Ortamları ve Çökeltmenin Evrimi. MTA Report No: 6306, 312 pp.
- Saner, S., 1980, Paleogeography and sedimentary environment of the Jurassic and younger sequences of the Mudurnu–Göynük basin: *Türkiye Jeoloji Kurumu Bülteni*, 23, 39–52.
- Sarı, A., and Aliyev, S.A., 2005, Source rock evaluation of the lacustrine oil shale bearing deposits: Göynük/Bolu, Turkey: *Energy Resources*, 27p, 279–298. DOI:10.1080/00908310490441980.
- Şengör, A.M.C., and Yılmaz, Y., 1981, Tethyan evolution of Turkey: A plate tectonic approach: *Tectonophysics*, 75, 181–241. DOI:10.1016/0040-1951(81)90275-4.
- Şeker, H., and Kesgin, Y., 1991, Nallıhan – Mudurnu – Seben – Beypazarı Arasında Kalan Bölgenin Jeolojisi ve Petrol Olanakları: TPAO Arama Grubu Başkanlığı no:2907, 42 pp [unpublished report in Turkish].
- Sherlock, S., Kelley, S., Inger, S., Harris, N., and Okay, A., 1999, 40 Ar–39 Ar and Rb–Sr geochronology of high-pressure metamorphism and exhumation history of the Tavşanlı Zone, NW Turkey: *Contributions to Mineralogy and Petrology*, 1371, 46–58.
- Tansel, İ., 1980, Nallıhan ve Dolayının Biyostratigrafi İncelemesi. *Yerbilimleri Dergisi*, Hacettepe Üniversitesi Yerbilimleri Uygulama ve Araştırma Merkezi, v. 5-6, 31–47 [in Turkish with English abstract].
- Timur, E., and Aksay, A., 2002, 1/100.000 Ölçekli Türkiye Jeoloji Haritaları. *Adapazarı- H26* Paftası İzahnamesi, Maden Tetkik

- Arama Genel Müdürlüğü Jeoloji Etütleri Dairesi, Ankara, 30, in Turkish with English abstract
- Turhan, N., 2002, 1/500.000 scale geological maps of Turkey-Ankara sheet, Mineral Research and Exploration (MTA) General Directorate, Ankara.
- Tüysüz, O., 1999, Geology of the Cretaceous sedimentary basins of the Western Pontides: *Geological Journal*, 341-2, 75–93. DOI:10.1002/(SICI)1099-1034(199901/06)34:1/2<75::AID-GJ815>3.0.CO;2-S.
- Wade, B.S., Pearson, P.N., Berggren, W.A., and Pälike, H., 2011, Review and revision of Cenozoic tropical planktonic foraminiferal biostratigraphy and calibration to the geomagnetic polarity and astronomical time scale: *Earth-Science Reviews*, 1041–3, 111–142. DOI:10.1016/j.earscirev.2010.09.003.
- Wolfring, E., Wagreich, M., Dinarès-Turell, J., Yılmaz, I.O., and Böhm, K., 2017, Plankton biostratigraphy and magnetostratigraphy of the Santonian–Campanian boundary interval in the Mudurnu–Göynük Basin, northwestern Turkey: *Cretaceous Research*, DOI:10.1016/j.cretres.2017.07.006.
- Yıldız, A., Kibici, Y., Bağcı, M., Dumlupınar, İ., Kocabaş, C., and Aritan, A.E., 2015, Petrogenesis of the post-collisional Eocene volcanic rocks from the Central Sakarya Zone (Northwestern Anatolia, Turkey): Implications for Source Characteristics, Magma Evolution, and Tectonic Setting. *Arabian Journal of Geosciences*, 812, 11239–11260.
- Yılmaz, İ.Ö., 2008, Cretaceous pelagic red beds and black shales (Aptian-Santonian), NW Turkey: Global Oceanic Anoxic and Oxidic Events: *Turkish Journal of Earth Sciences*, 172, 263–296.
- Yılmaz, İ.O., Altın, D., and Ocakoğlu, F., 2016, Upper Jurassic–Lower Cretaceous depositional environments and evolution of the Bilecik (Sakarya Zone) and Tauride carbonate platforms, Turkey: *Palaeogeography, Palaeoclimatology, Palaeoecology*, 449, 321–340. DOI:10.1016/j.palaeo.2016.02.028.